Einleitung

BildVERarbeitung

- Bildanalyse
- Bildrestauration
- Photometrische Auswertung
- Objektdetektion
- Kompression
- …

BildBEarbeitung

- „Astrofotografie“
- Farbkanäle gezielt manipulieren
- …

Einleitung

Astronomische Bildverarbeitung

Filterung
- Image Denoising (Entfernen von Bildrauschen, Photometrie)
- Kontrastverbesserung
- …

Deconvolution („Bildschärfung“)
- Inverse Filterung
- Regularisierung
- Statistische Methoden (Bayes, Entropie,…)
- Super-Resolution
- …

Bildkomprimierung
- Übermitteln von Daten (Sonden), Bilddatenbanken

Compressed Sensing

usw. …

CCD-Kamera Charakterisierung

Noise characteristics of CCD camera

Total standard deviation $<n_{camera}>$ of camera noise:

$$< n_{Camera} > = \sqrt{< n^2{}_{shot} > + < n^2{}_{read} > + < n^2{}_{pattern} >}$$

Pattern noise (fixed pattern noise and photoresponse non-uniformities) manifests as a spatial non-uniformity

Poisson-noise (quantum nature of light)

$$P(X = x) = \frac{m^x e^{-l}}{x!}$$

E(X) = l ,   Var(X) = l

where l is the average number of occurrences
(e.g. number of generated photo-electrons on the CCD)

Gaussian read-out-noise (camera electronics)

Var(X) = const.

CCD-Kamera Charakterisierung

Noise characteristics of CCD camera

Photon transfer technique

- **Conversion of photon numbers to CCD gray levels**

- Plot of random noise as a function of mean signal.

- It gives the conversion constant used to convert relative digital units generated by the camera into absolute physical units of electrons/photons.

- As the illumination onto the CCD is increased, the noise becomes dominated by the shot noise/photon noise associated with the random arrival of photons

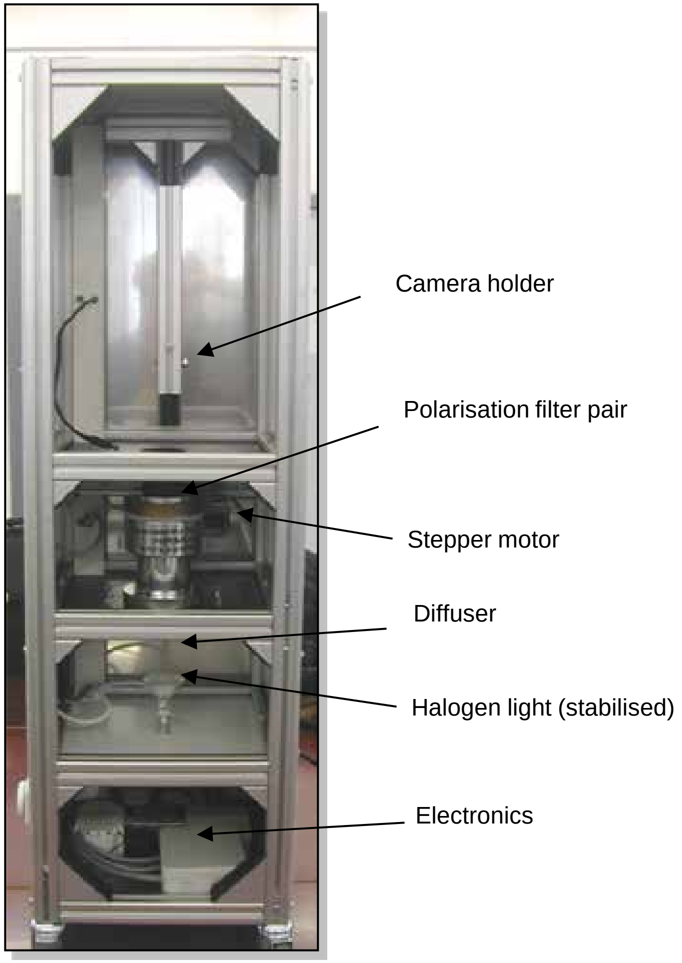

Fig.2: Measurement device for PTC

CCD-Kamera Korrekturen

Flatfield-Korrektur

Eine radiometrische Korrektur bei der individuelle Pixelwerte korrigiert werden, wird als ‚Flat fielding' (bzw. ‚Shading correction') bezeichnet. Die Flatfield-Korrektur (nach [29], [30]) korrigiert Inhomogenitäten die aufgrund systematischer Fehler durch Background noise und Pattern noise (siehe Kap.7.6) entstehen. Die allgemeine Struktur dieser Korrektur kann folgendermaßen angeschrieben werden:

$$p_c = (p - offset) * gain$$

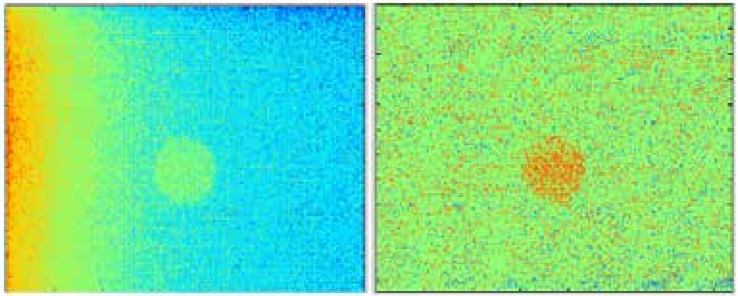

Abb. 8.4: Aufnahme einer schwachen Lichtquelle (Zentrum) ohne (links) und mit Dunkelbildkorrektur (rechts).

Bildvorverarbeitung

„Image Stacking“

Verbesserung des SNR!

Bildvorverarbeitung

„Drizzle“

Superresolution / dithering

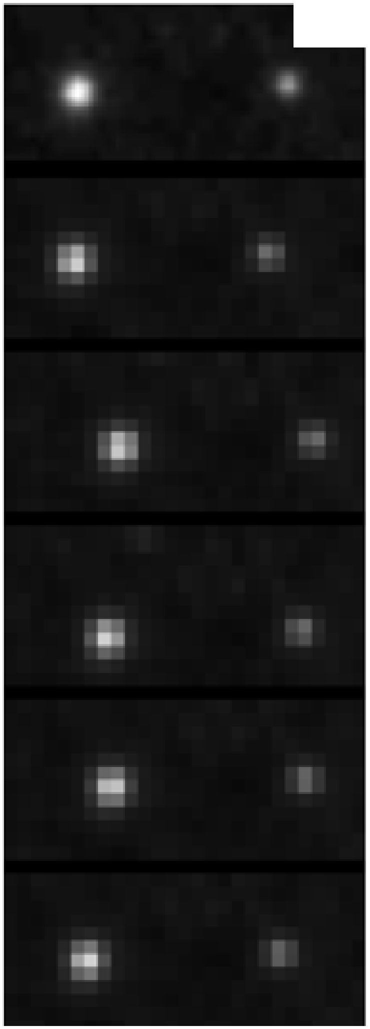

Image Denoising

Image Denoising

Linear Filtering

Degree of smoothing depends on size of filter kernel

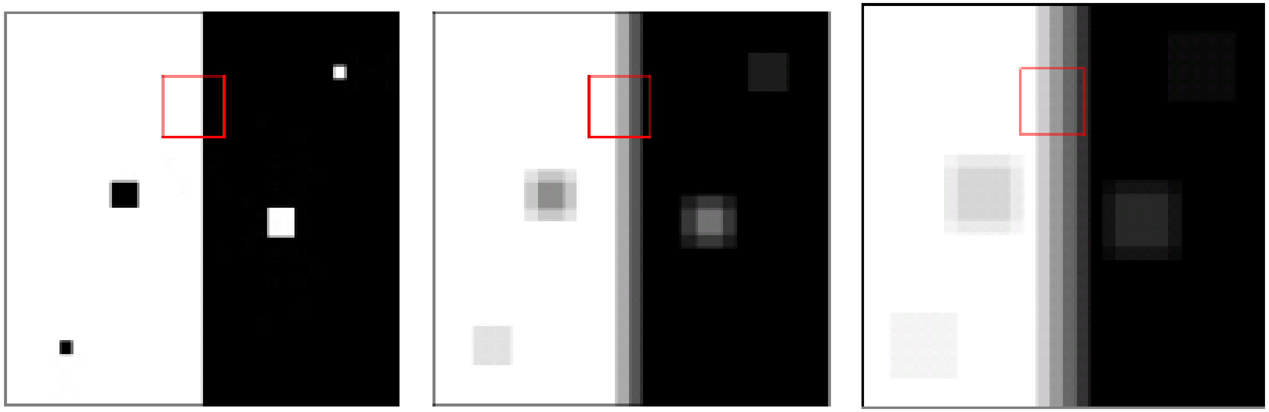

3x3, 5x5 and 7x7 filter kernel

Image Denoising

Image transform

FOURIER transform

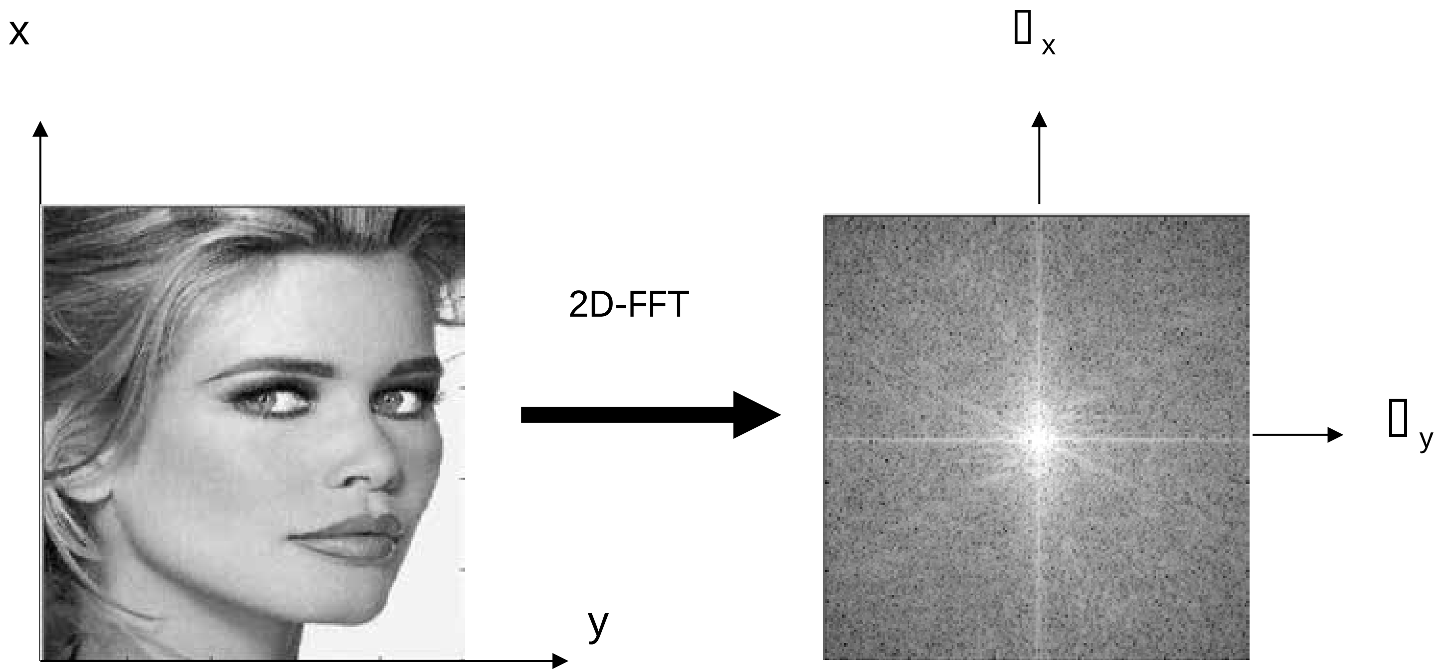

Ortsraum

(Orts-)Frequenzraum

Image Denoising

Image transform

FOURIER transform

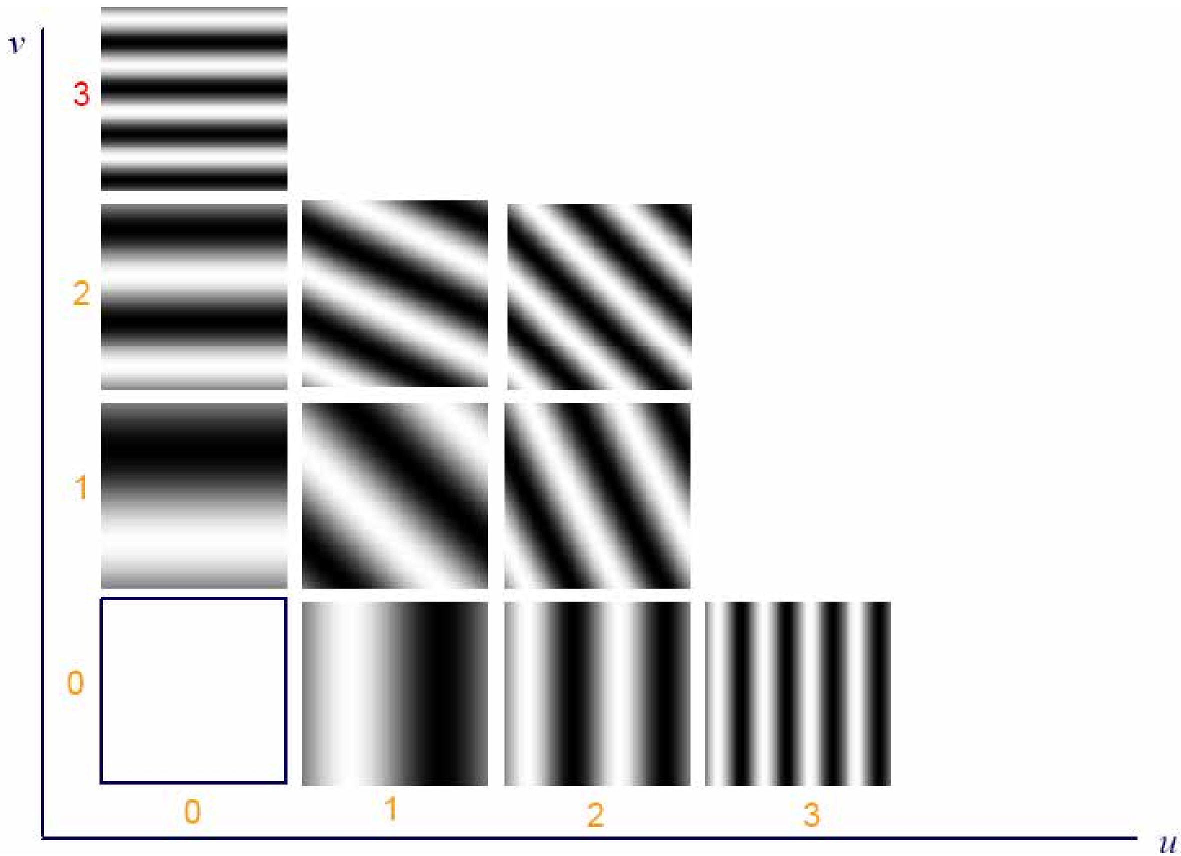

Image Denoising

Image transform

WAVELET transform

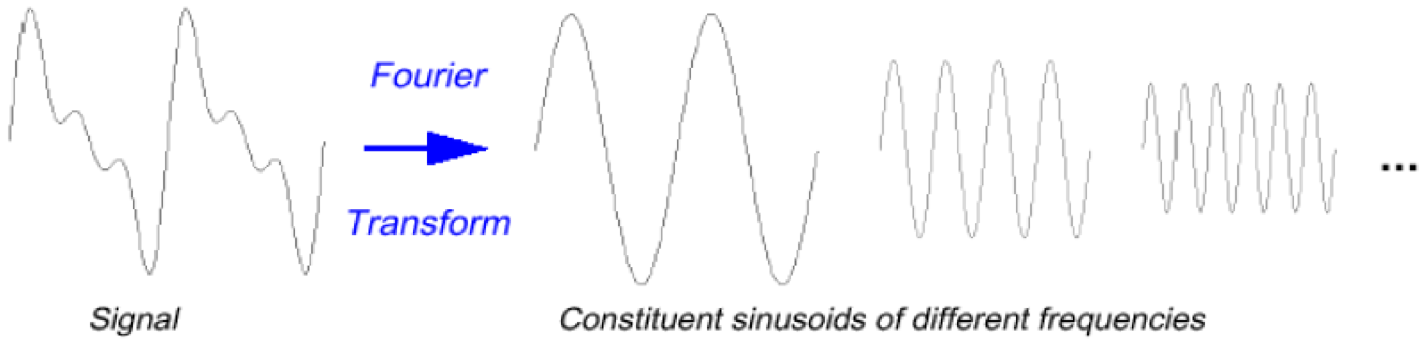

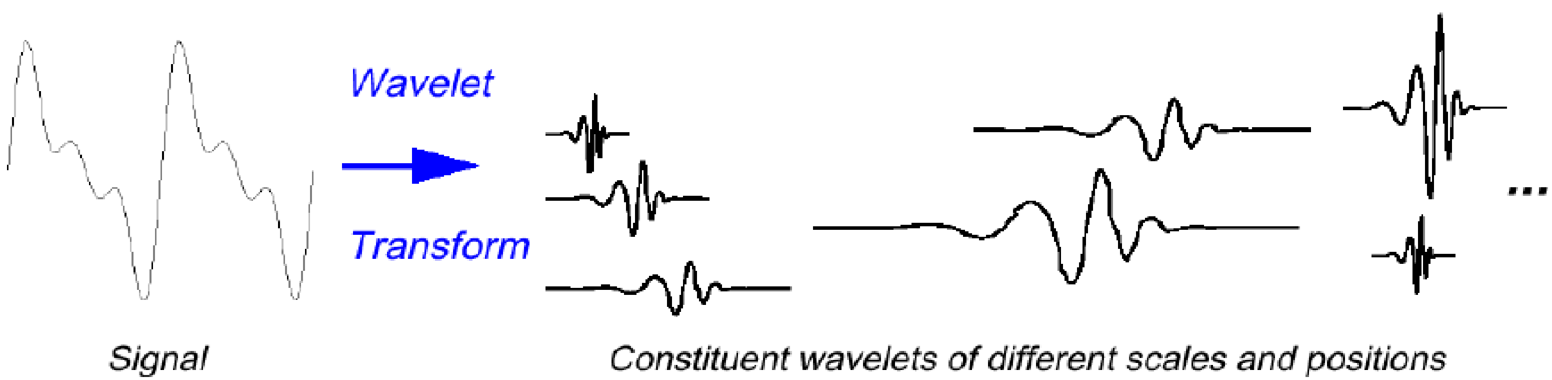

Image Denoising

MULTIRESOLUTION

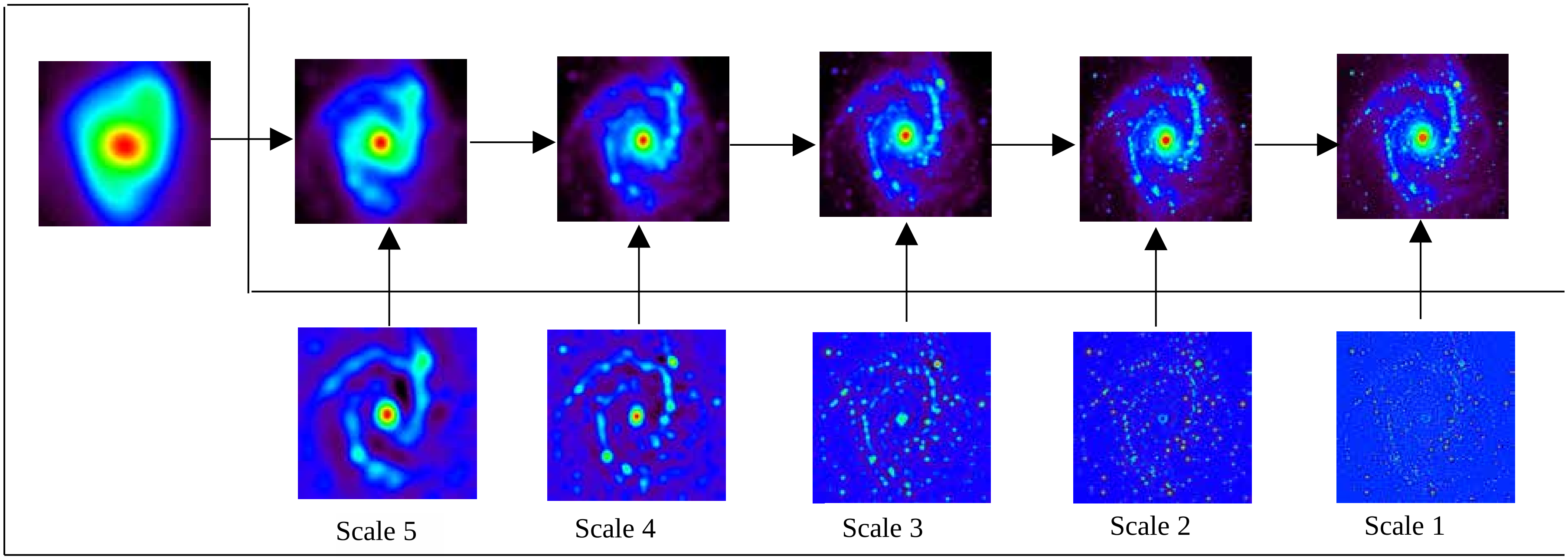

Image Denoising

density/intensity estimate

NEWTON/XMM Image
of the supernovae SN1604

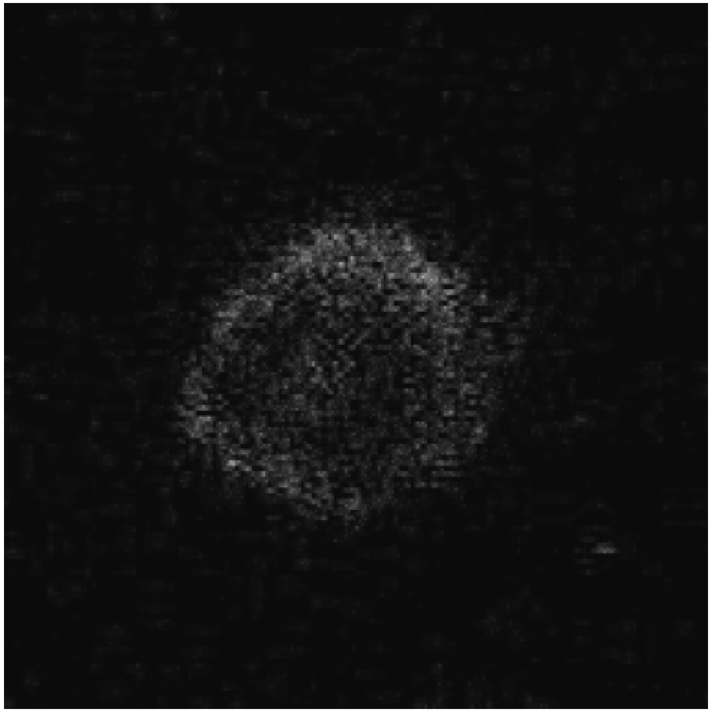

„photon limited imaging“

Ridgelet Filtering

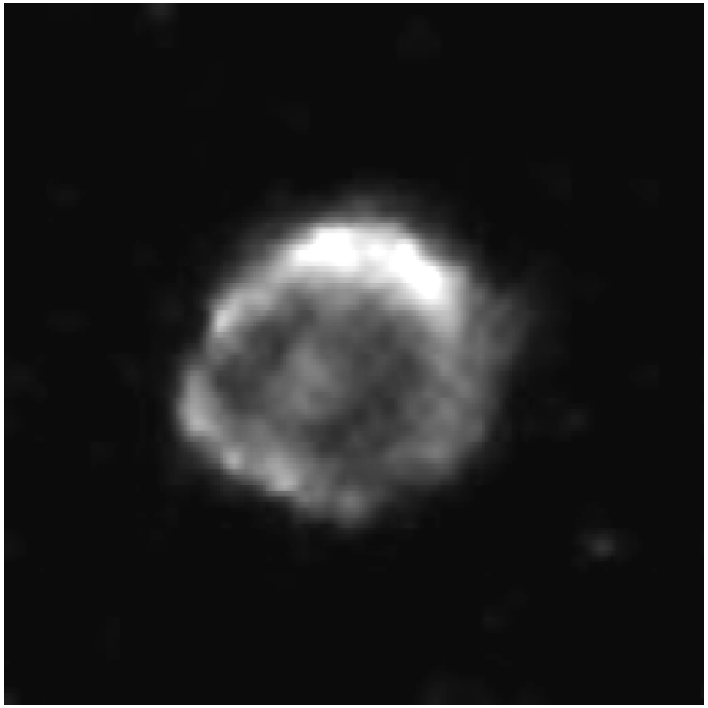

Image Denoising

density/intensity estimate

„photon limited imaging“

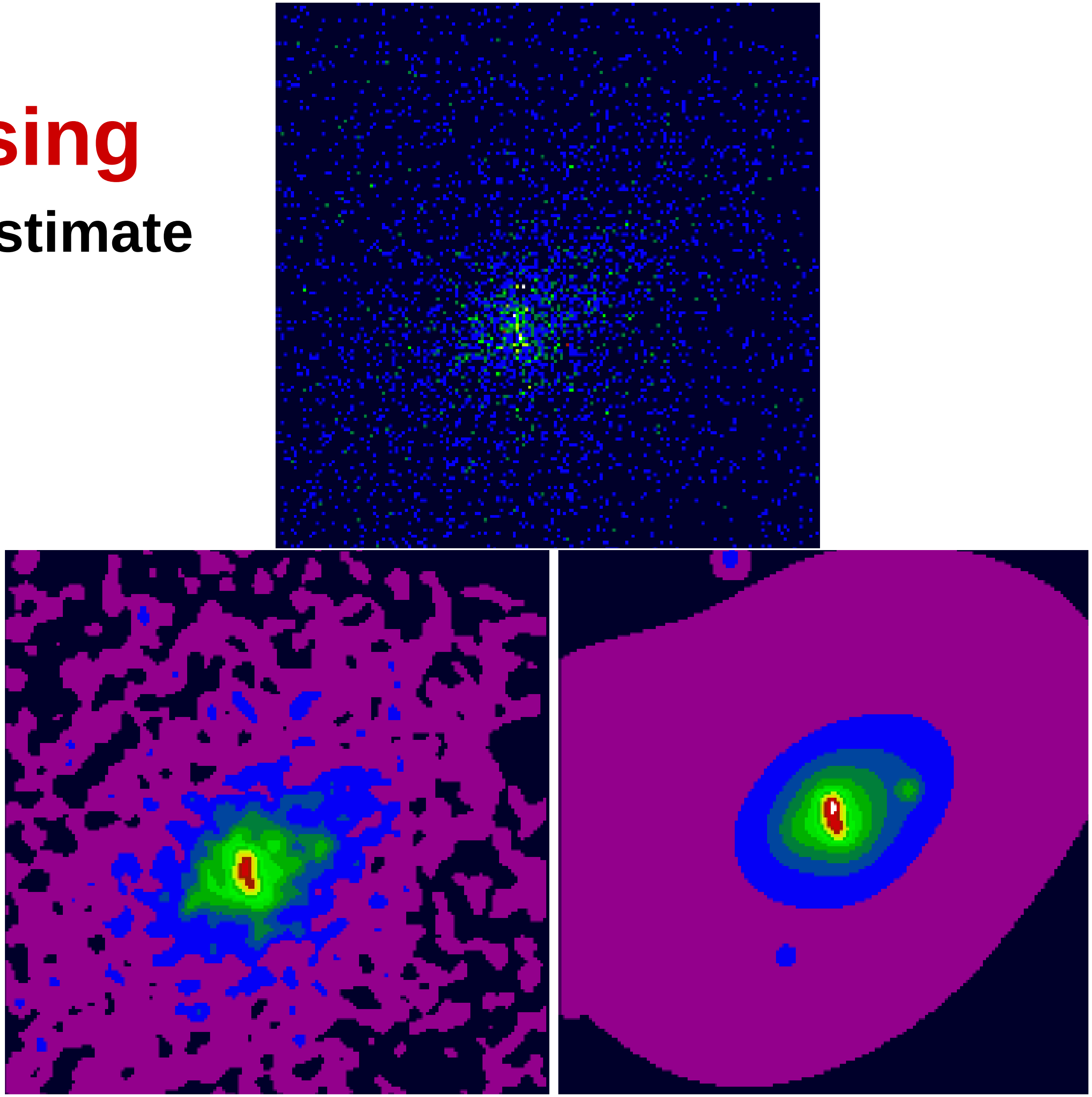

Fig. 2.12. Top, ROSAT image of the cluster A2390. Bottom left, ROSAT image of the cluster A2390 filtered by the standard method (convolution by a Gaussian). Bottom right, ROSAT image of the cluster A2390 filtered by the method based on wavelet coefficients.

Image Denoising

density/intensity estimate

„photon limited imaging"

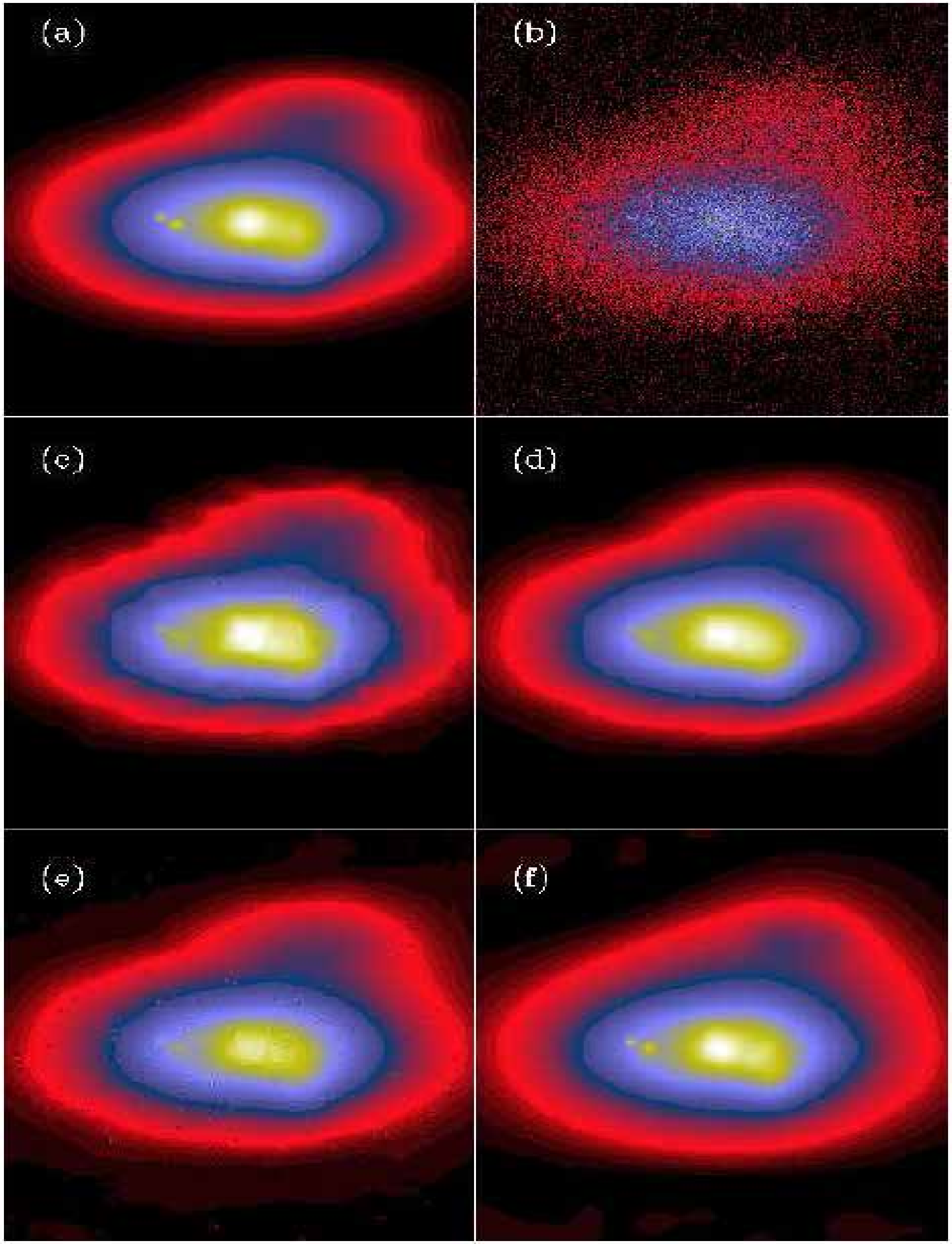

Fig. 2.14. Top, simulated galaxy cluster and simulated data. Middle, Haar-Kolaczyk filtered images using the undecimated Haar transform and the undecimated bi-orthogonal Haar transform. Bottom, Haar-Jammal-Bijaoui filtered image and the à trous algorithm.

Image Denoising

„Dictionary Learning“

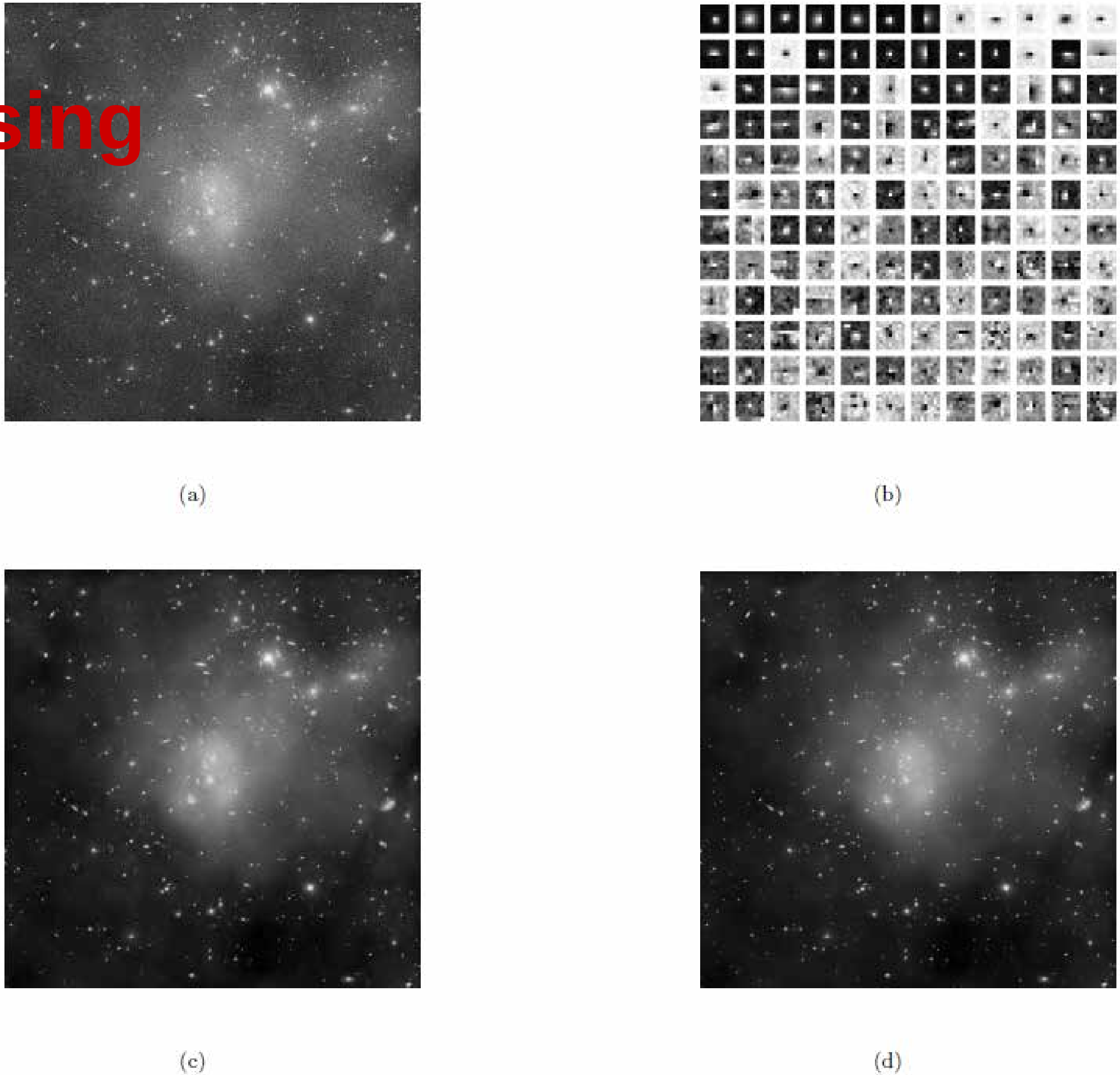

Figure 2. Results of denoising with galaxy cluster image. Figure (a) shows the image noisy image, with a PSNR of 26.52 dB. The learned dictionary is shown Figure (b). Figure (c) shows the result of the wavelet shrinkage algorithm that reaches a PSNR of 38.92 dB, Figure (d) shows the result of denoising using the dictionary learned on the noisy image, with a PSNR of 39.35 dB.

Image Denoising

„Dictionary Learning“

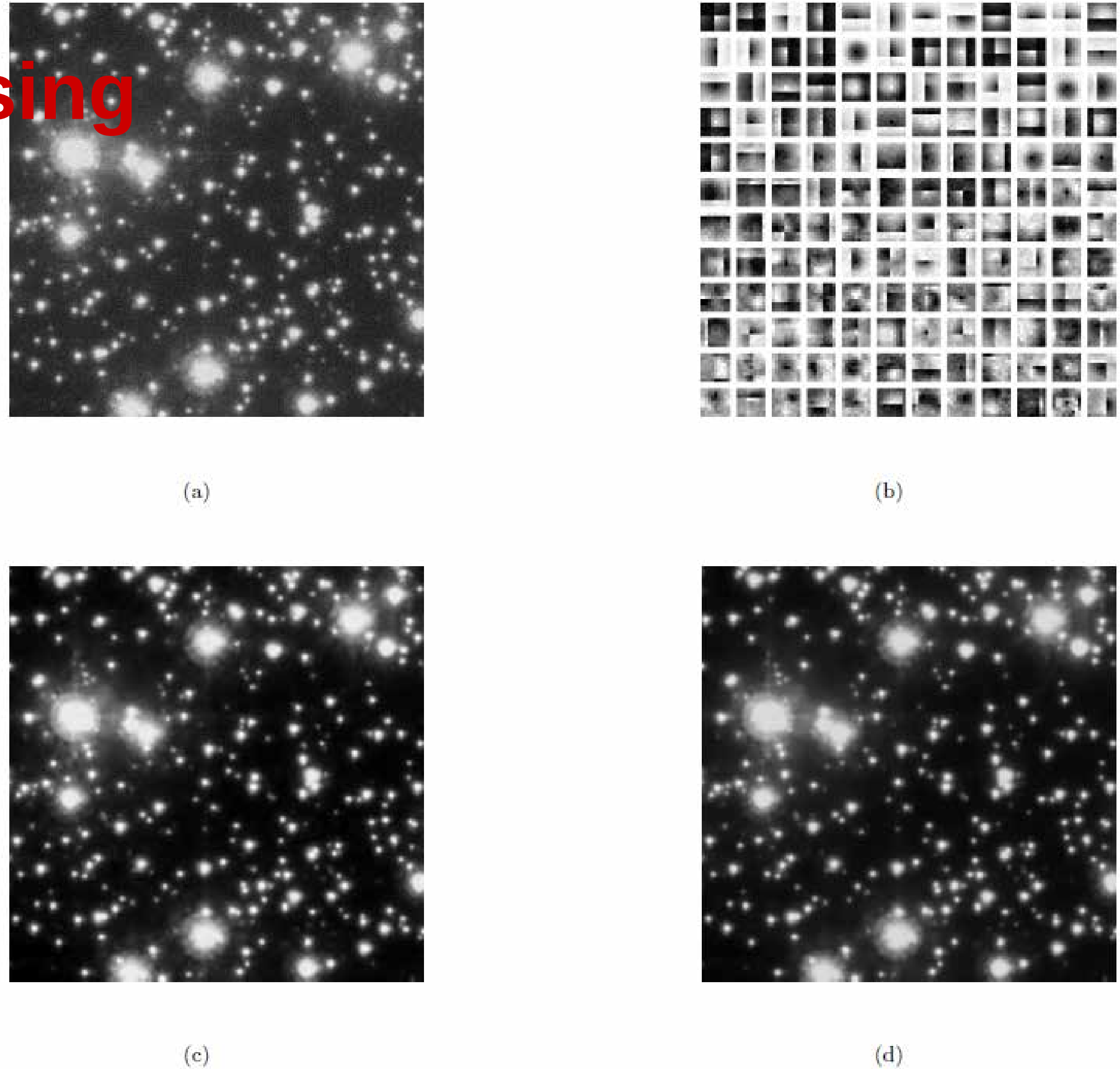

Figure 3. Results of denoising with star cluster image. Figure (a) shows the image noisy image, with a PSNR of 27.42 dB. The learned dictionary is shown Figure (b). Figure (c) shows the result of the wavelet shrinkage algorithm that reaches a PSNR of 37.28 dB, Figure (d) shows the result of denoising using the dictionary learned on the noisy image, with a PSNR of 37.87 dB.

Deconvolution

Deconvolution

(“Bildschärfung”)

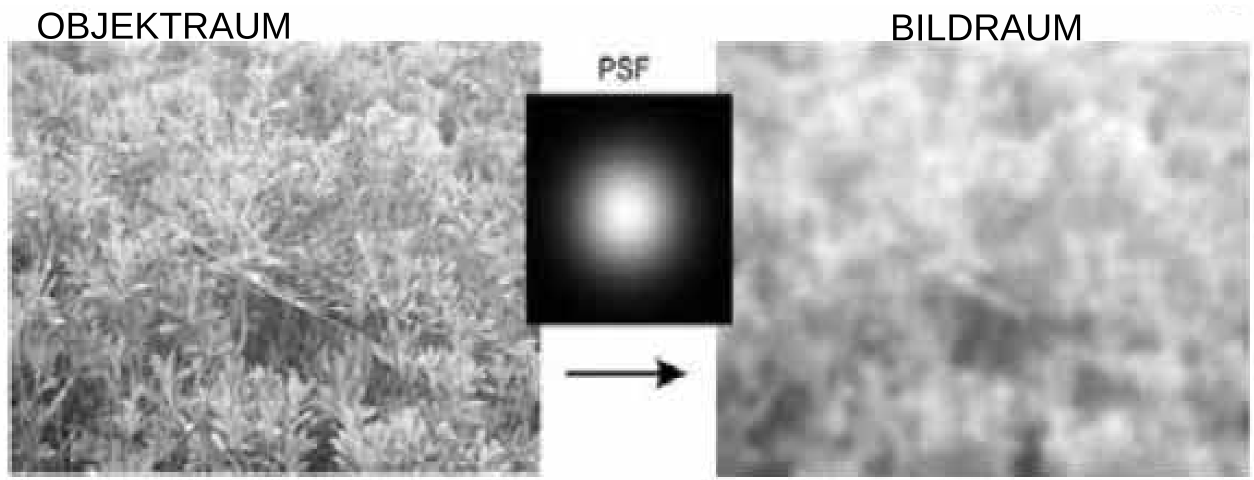

„perfektes“ Bild

PSF
(Punktverschmierungsfunktion)

„unscharfes“ Bild

Ein Punkt im Objektraum wird nicht auf einen Punkt im Bildraum abgebildet, sondern auf eine mehr oder weniger ausgedehnte Fläche variierender Intensität.

Deconvolution

(“Bildschärfung”)

Point Spread Function (PSF) in Astronomy

$$I_{observed} = I_{real} \otimes PSF$$

- Easy to measure and model from several stars usually present in astro-images
- Determines the spatial resolution of an image
- Commonly used for image matching and deconvolution

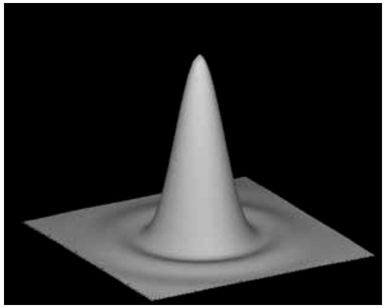

Ideal PSF if no atmosphere
FWHM ~ 1.22 x l /D
→ < 0.1" (8m telescope)

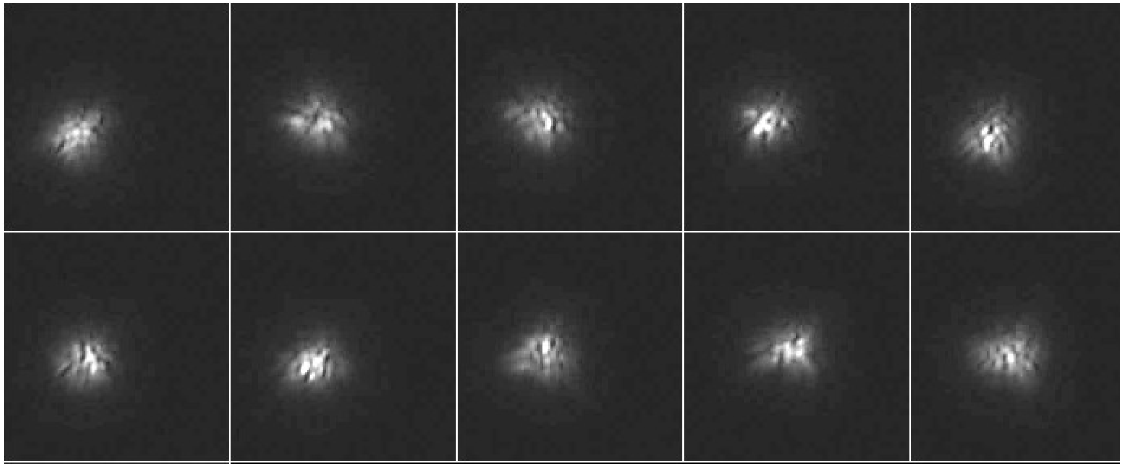

Atmospheric turbulence broadens the PSF
→ Gaussian PSF with FWHM ~ 1"

Deconvolution

("Bildschärfung")

Point Spread Function (PSF) in Astronomy

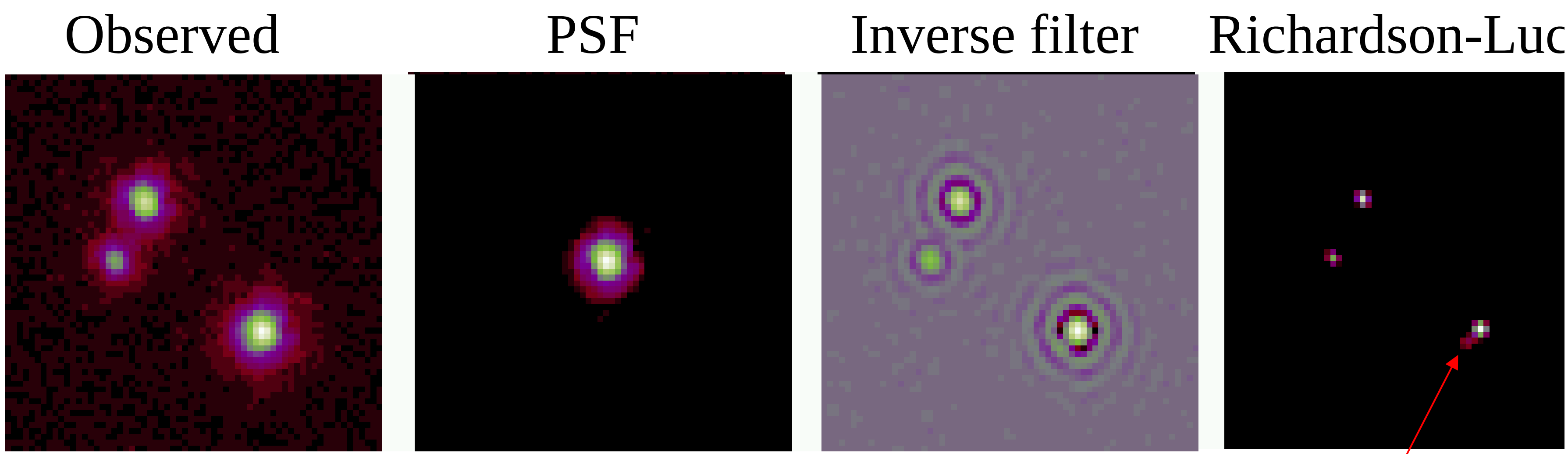

Problem: not constant over time!

4th object!

Deconvolution

Image Restoration

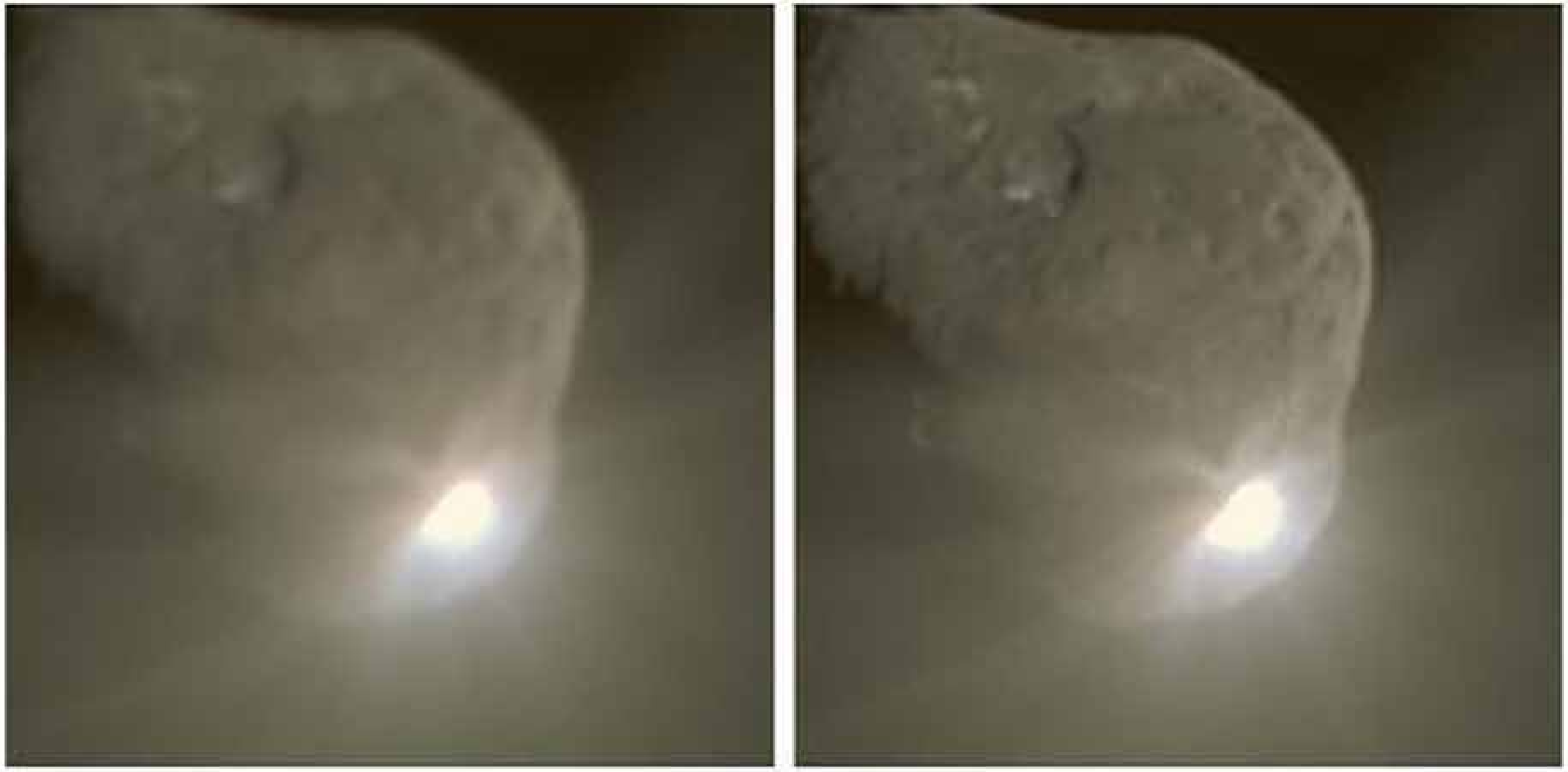

Fig. 3.4. Deep Impact image (*left*) and deconvolved image (*right*) using the Richardson-Lucy method.

Deconvolution

Image Restoration

MATLAB image processing toolbox!

PSF

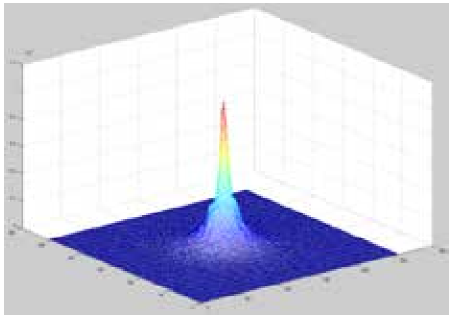

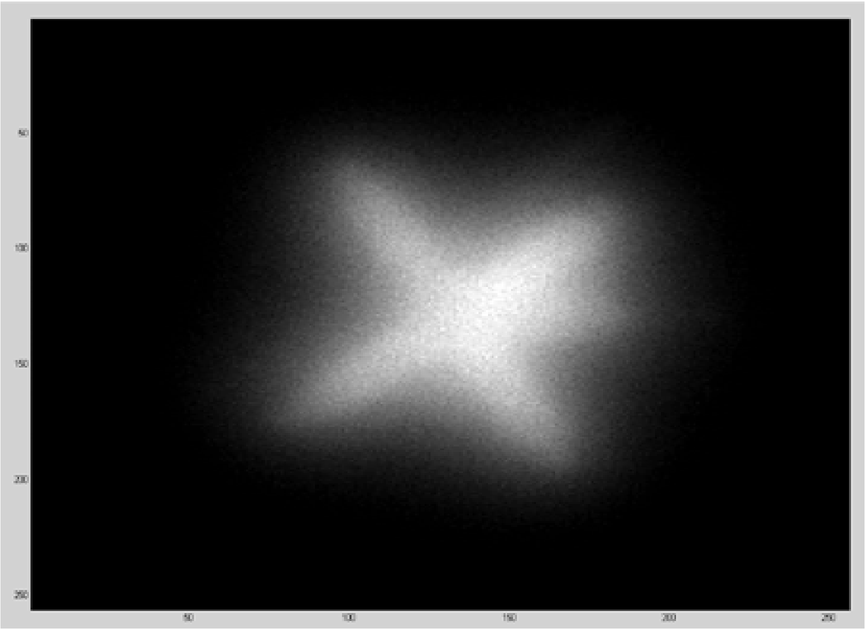

original

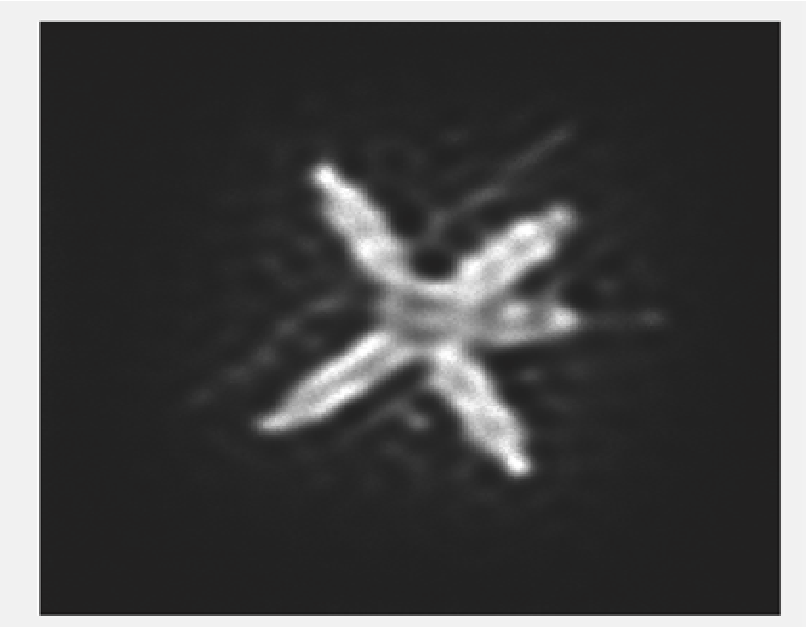

deblurred

Deconvolution

Image Restoration

Wavelet based results

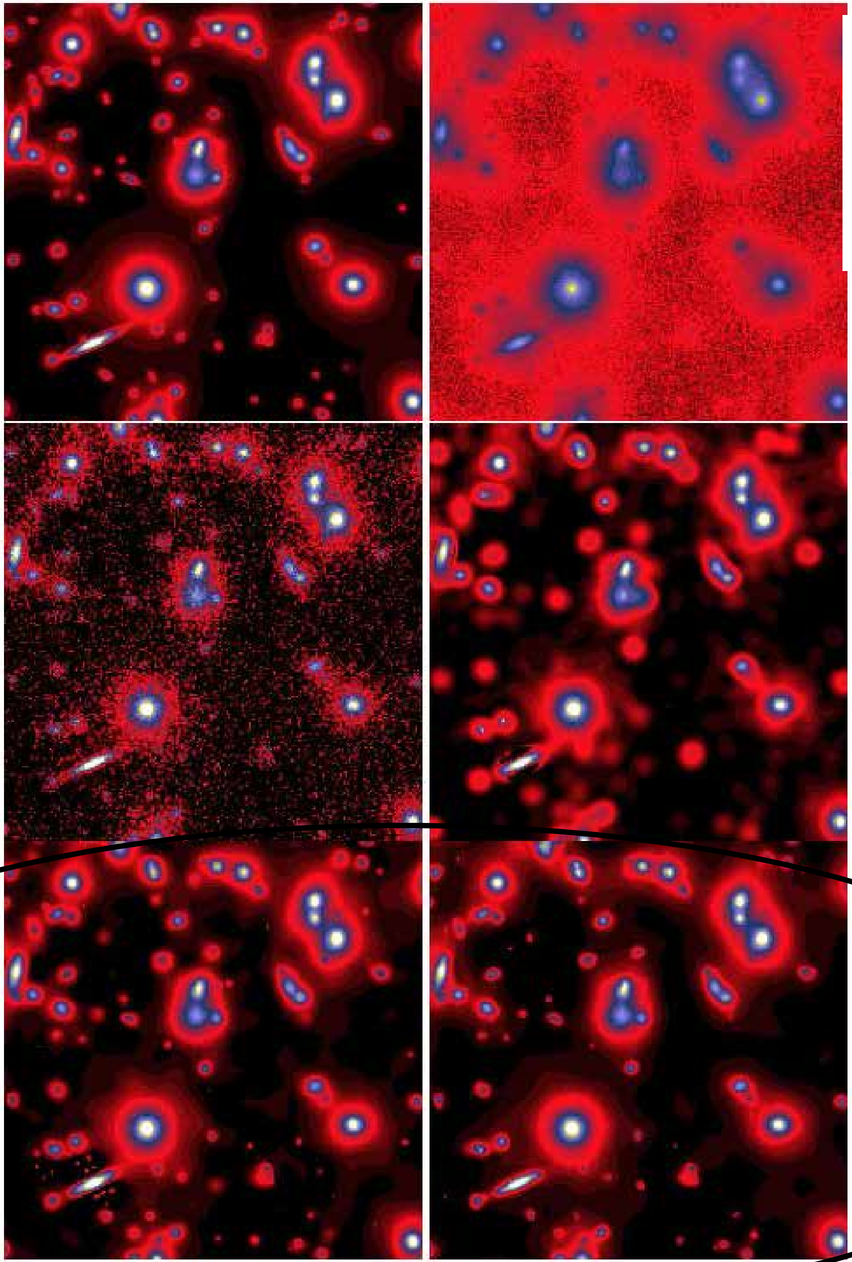

Fig. 3.6. Simulated Hubble Space Telescope Wide Field Camera image of a distant cluster of galaxies. Six quadrants. Upper left: original, unaberrated and noise-free. Upper right: input, aberrated, noise added. Middle left: restoration, Richardson-Lucy. Middle right: restoration, Pixon method. Lower left, restoration wavelet-vaguelette. Lower right, restoration wavelet-Lucy.

Deconvolution

Image Restoration

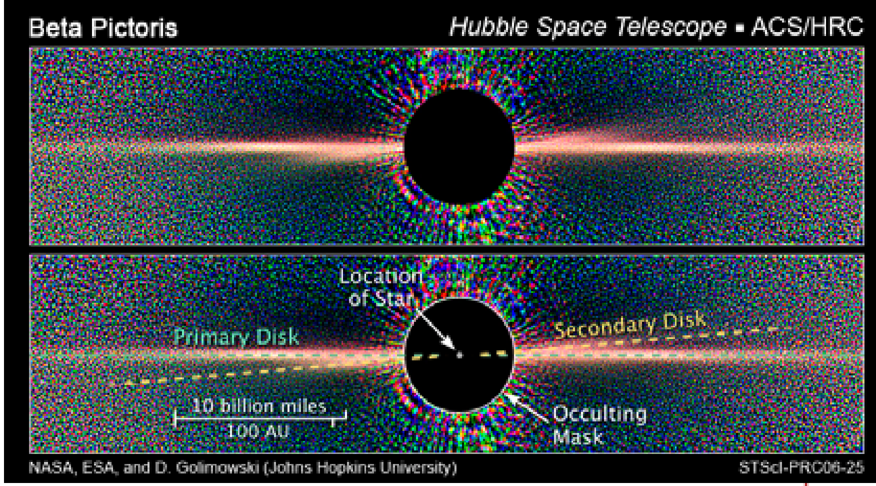

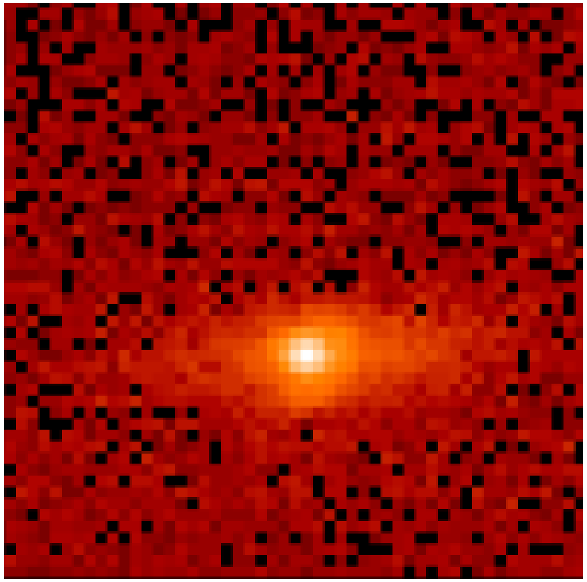

Fig. 3.10. Beta Pictoris raw data.

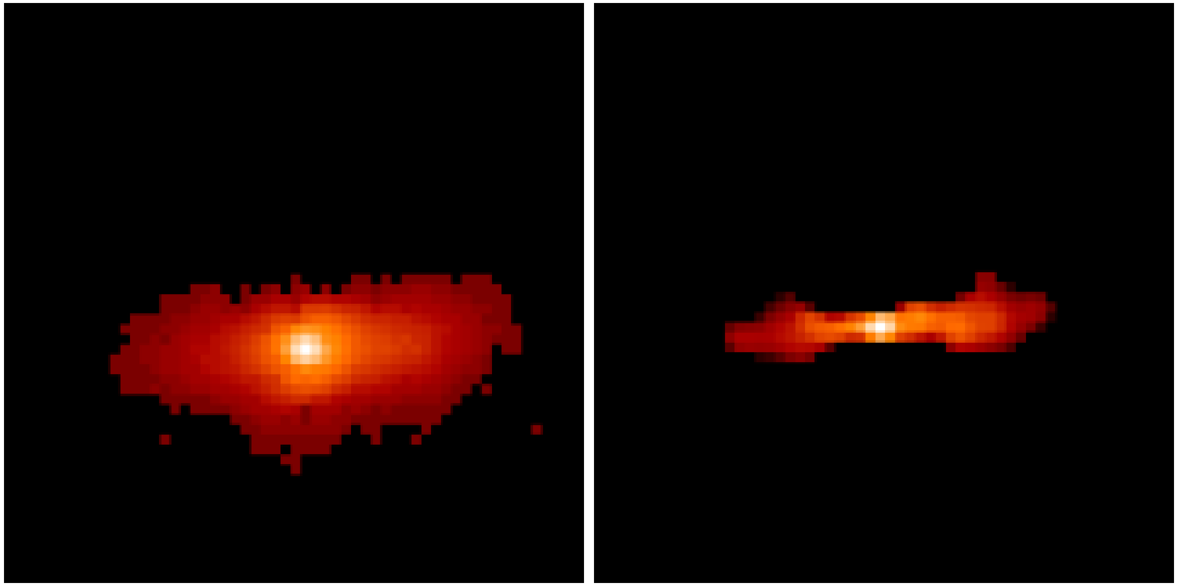

Fig. 3.11. Filtered image (left), and deconvolved one (right).

Deconvolution

Image Restoration

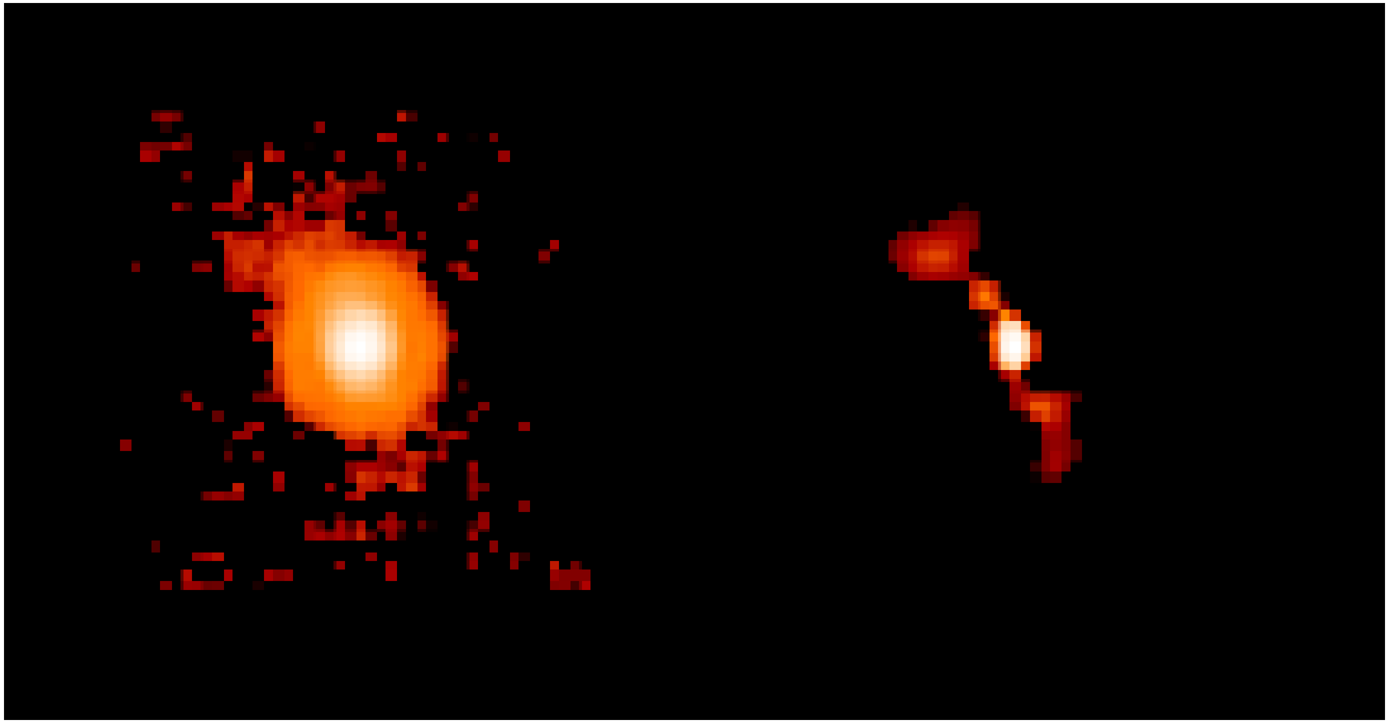

Fig. 3.1. The active galaxy nucleus of NGC1068 observed at 20 μm. Left: the raw image is highly blurred by telescope diffraction. Right: the restored image using the multiscale entropy method reveals the inner structure in the vicinity of the nucleus.

Deconvolution

Image Restoration

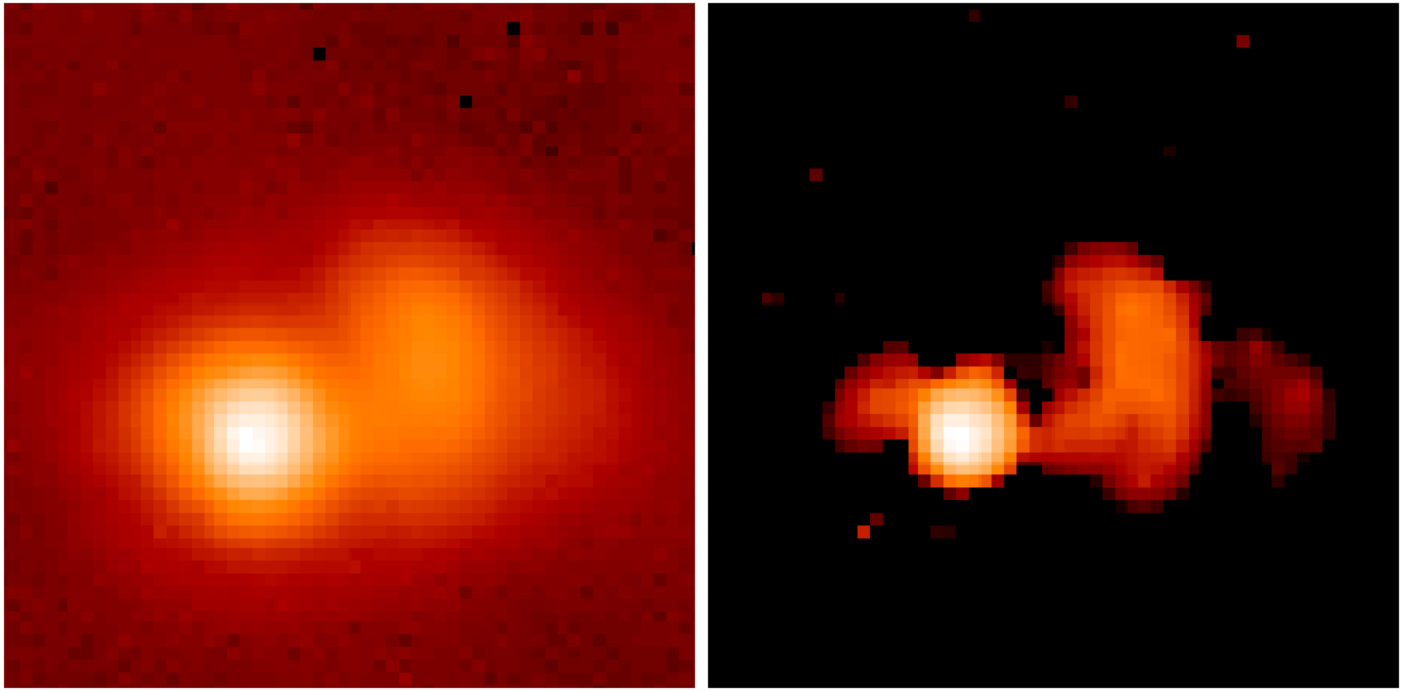

Fig. 3.2. The young stellar object AFGL4029 observed with various instruments

Detection

Detection

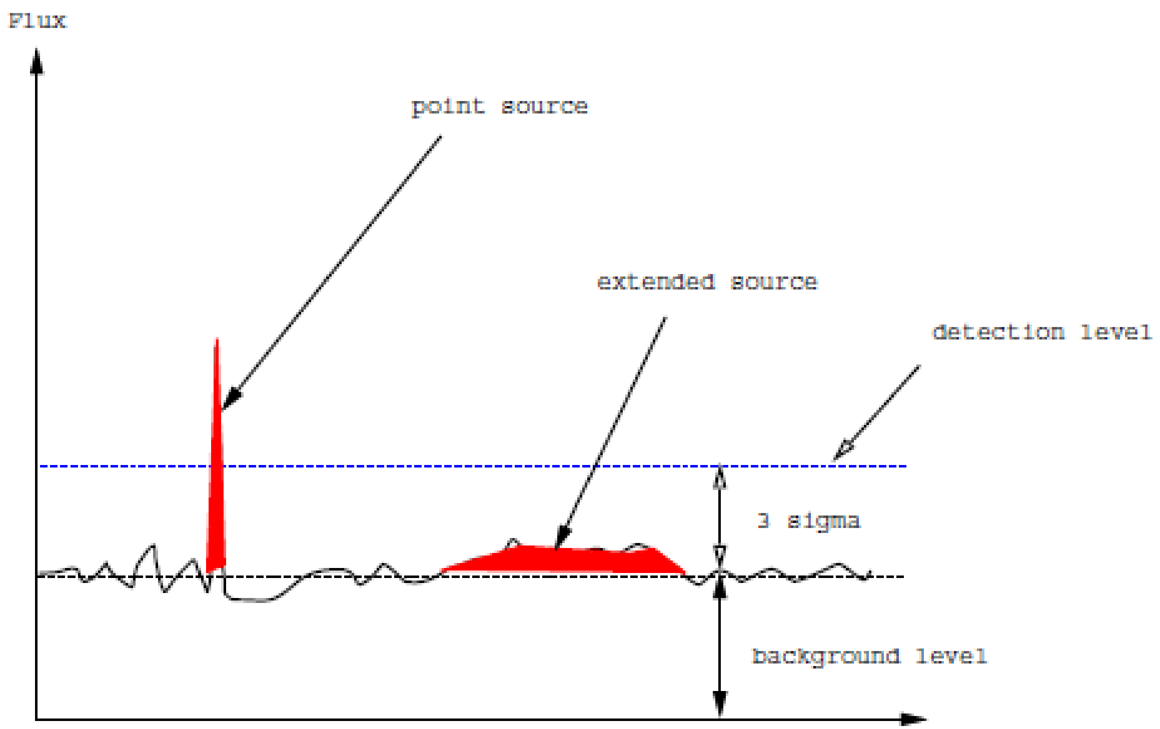

Fig. 4.1. Example of astronomical data: a point source and an extended source are shown, with noise and background. The extended object, which can be detected by eye, is undetected by a standard detection approach.

Detection

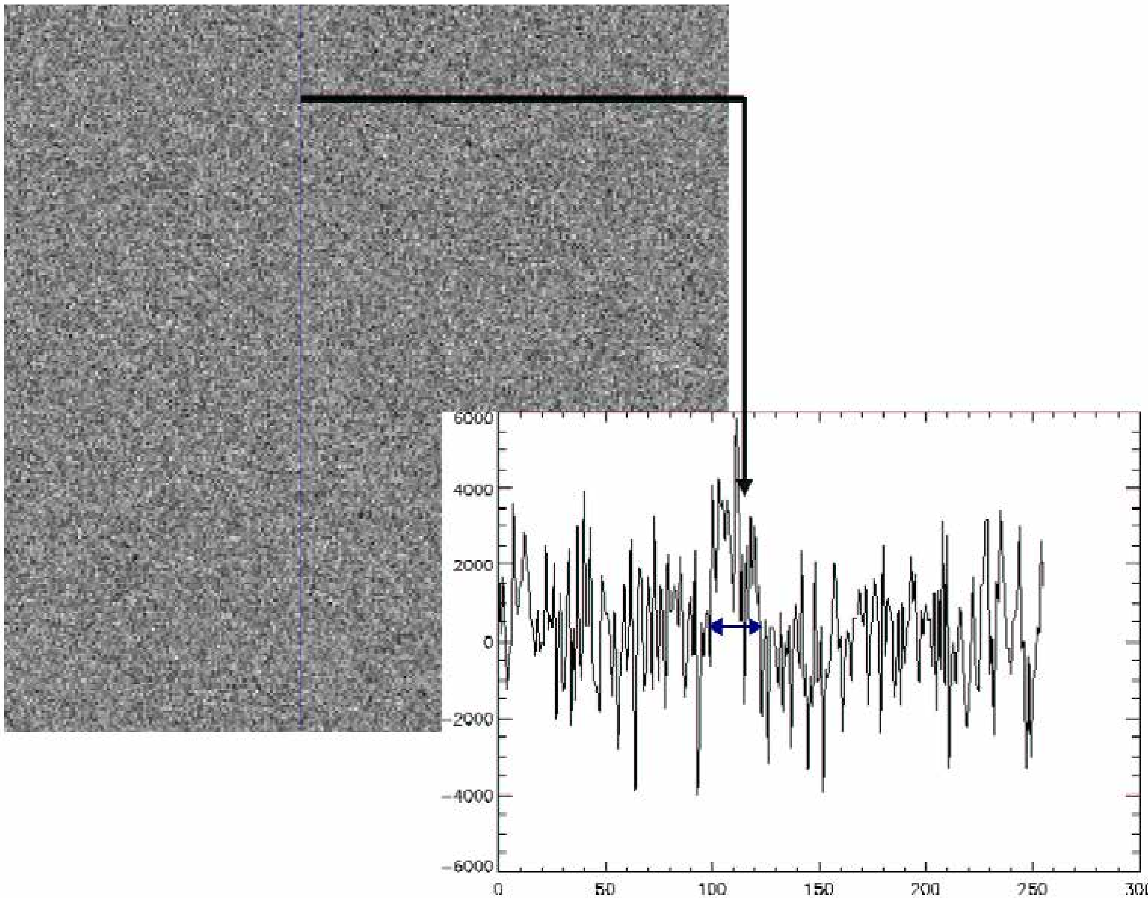

Detection

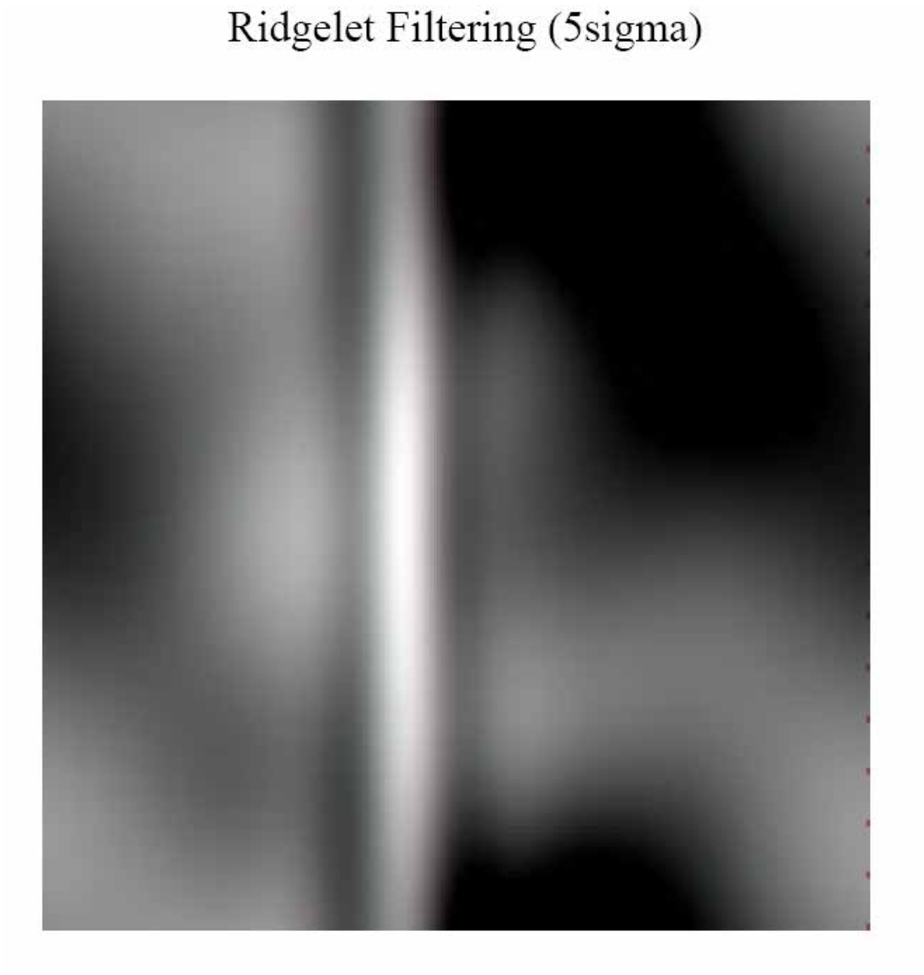

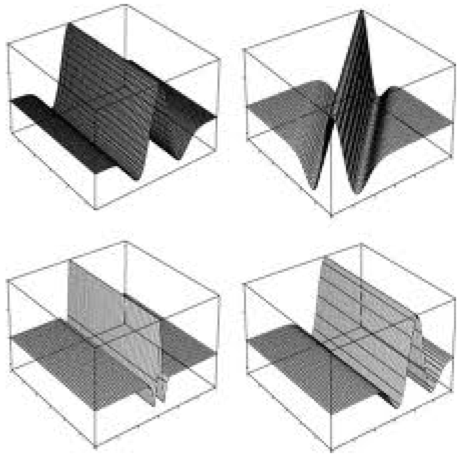

Detection

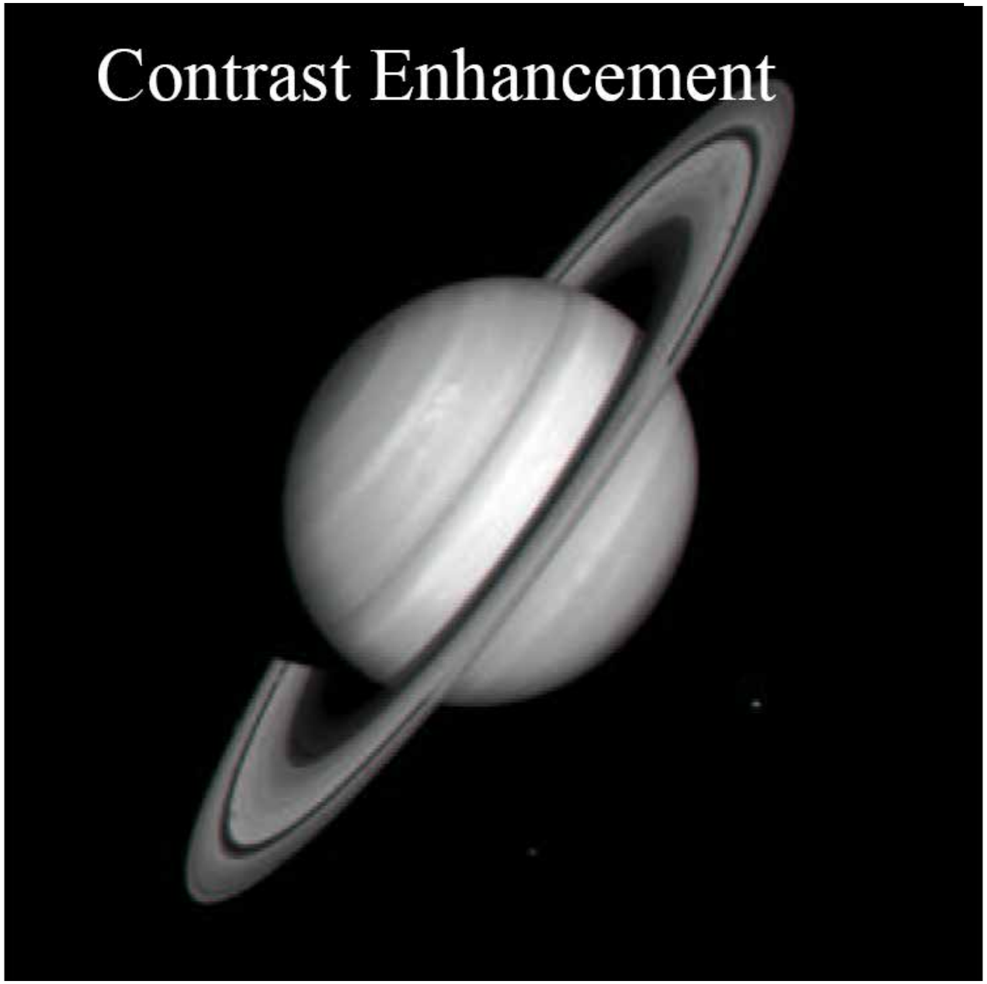

Detection

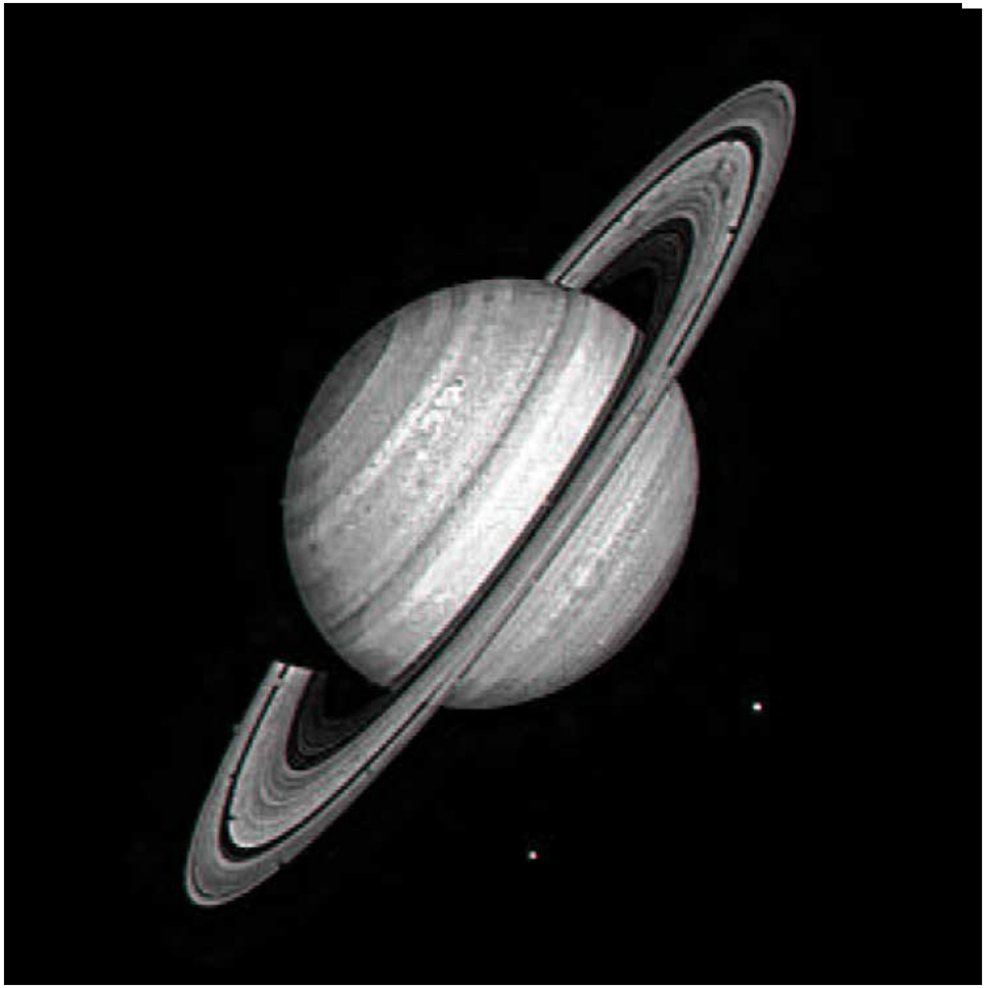

Detection

Object Identification

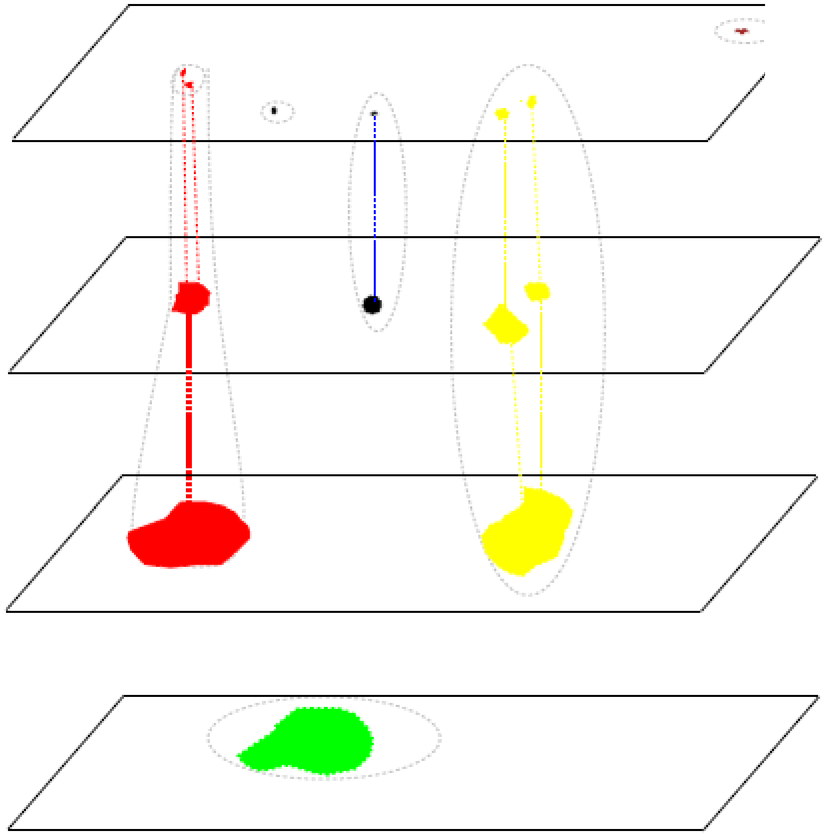

Fig. 4.2. Example of connectivity in wavelet space: contiguous significant wavelet coefficients form a structure, and following an interscale relation, a set of structures forms an object. Two structures S_j, S_{j+1} at two successive scales belong to the same object if the position pixel of the maximum wavelet coefficient value of S_j is included in S_{j+1}.

Detection

Object Identification

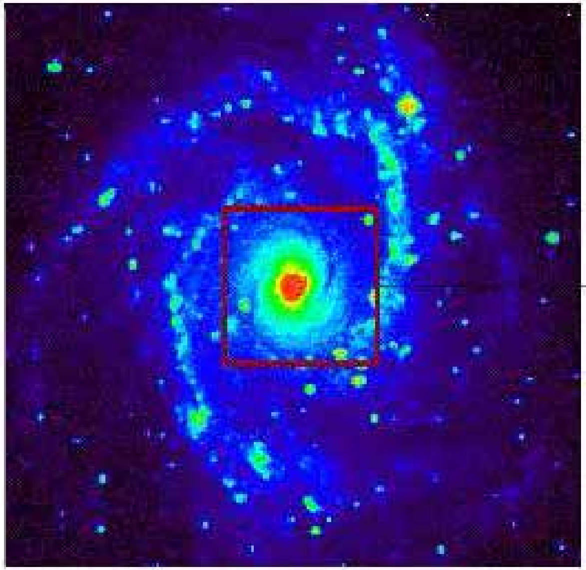

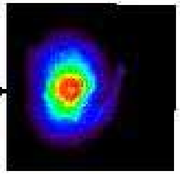

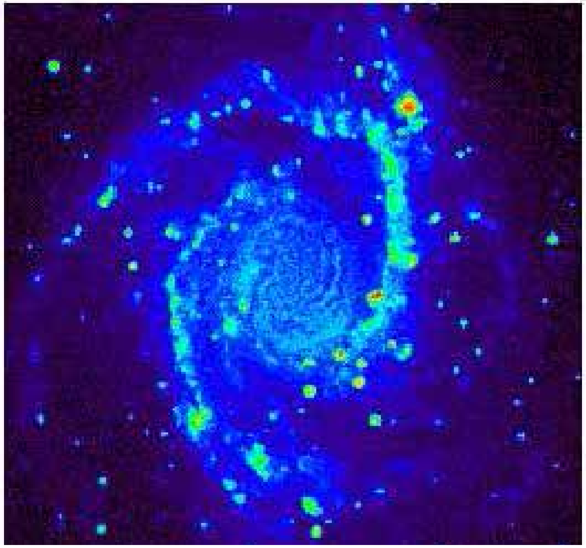

Detection

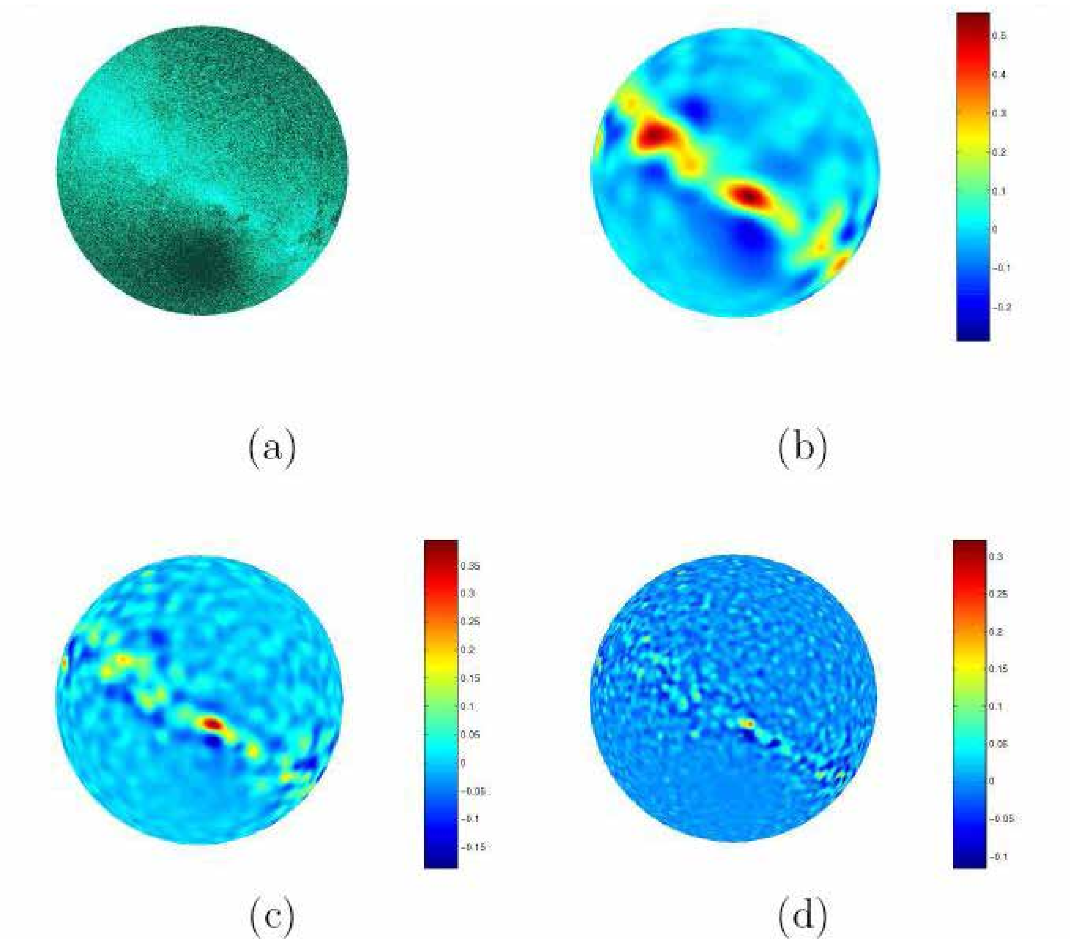

„wavelets on the sphere"

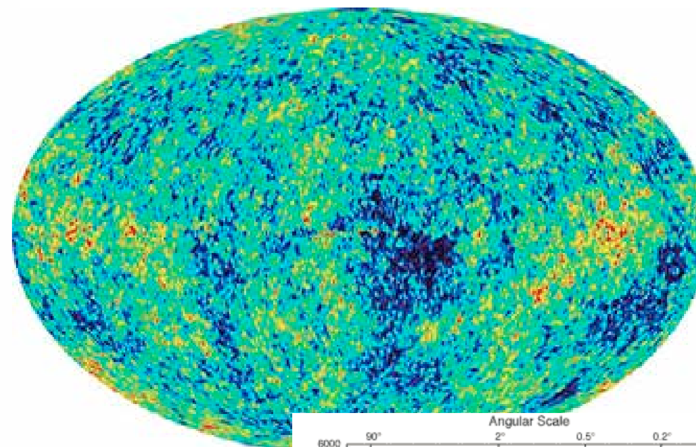

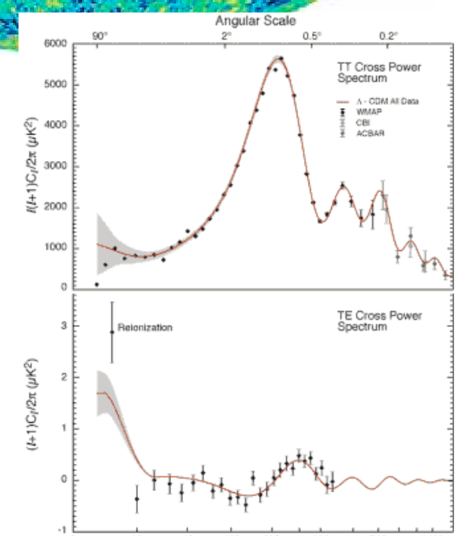

Compression

Compression

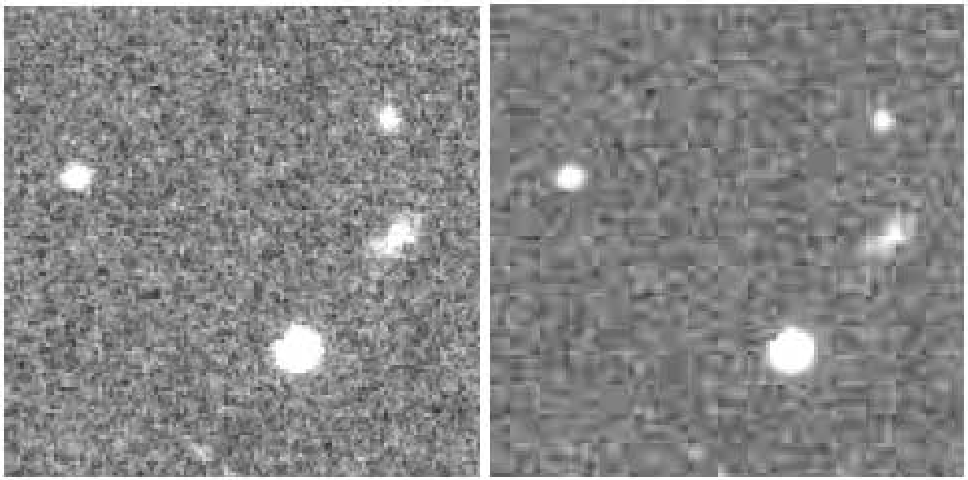

Fig. 5.4. Left: Original image, subimage extracted from 1024×1024 patch, extracted in turn from the central region of ESO7992v. Right: JPEG compressed image at 40:1 compression rate.

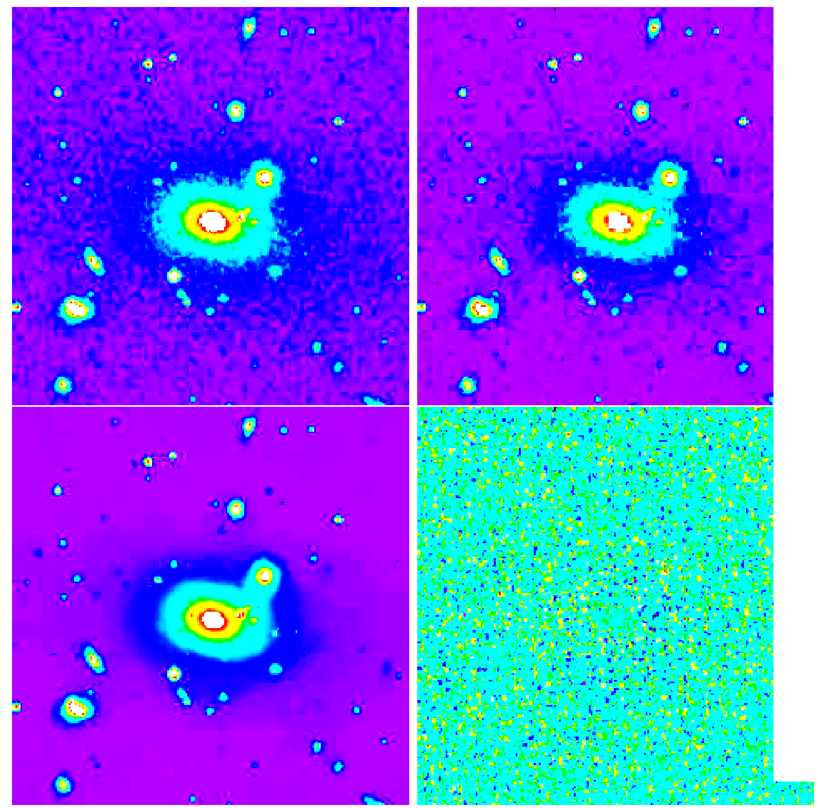

Fig. 5.2. Upper left. Coma cluster from a Space Telescope Science Institute POSS-I digitized plate. Upper right. decompressed image using HCOMPRESS (30:1). Bottom left. decompressed image using Pyramidal Median Transform (30:1). Bottom right. difference between the original image and the PMT decompressed one.

Compression

Bildkompression

519 FFT-Koeffizienten

532 WVLT-Koeffizienten

Compression

Information - Entropie

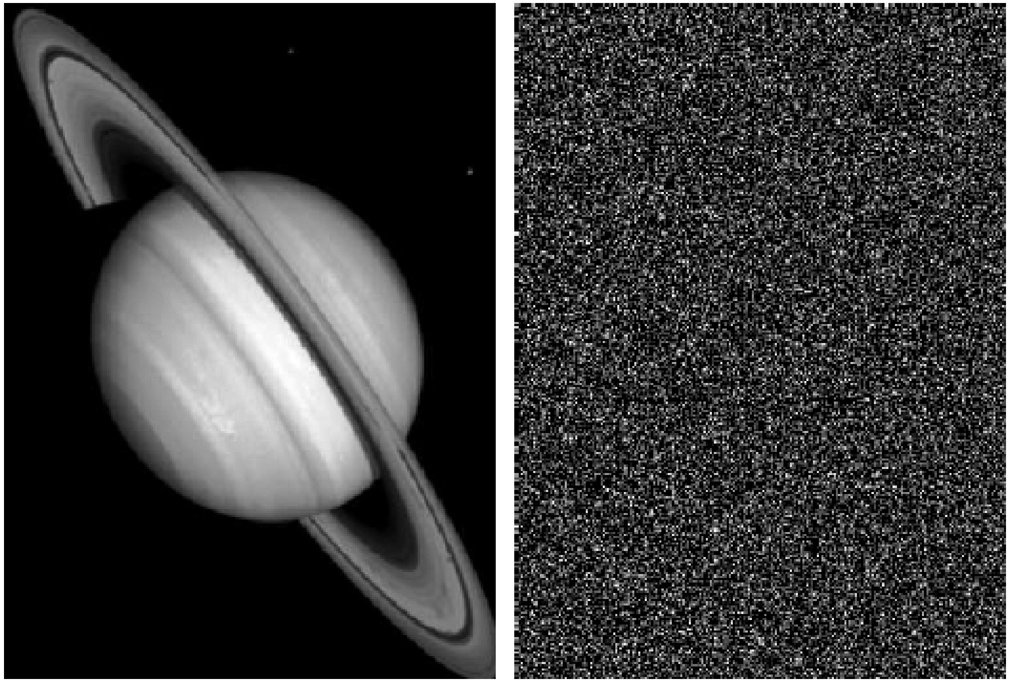

Fig. 7.1. Saturn image (left) and the same data distributed differently (right). These two images have the same entropy using any of the standard entropy definitions.

Compression

Information - Entropie

$$H = -\sum_i p_i \ln(p_i)$$

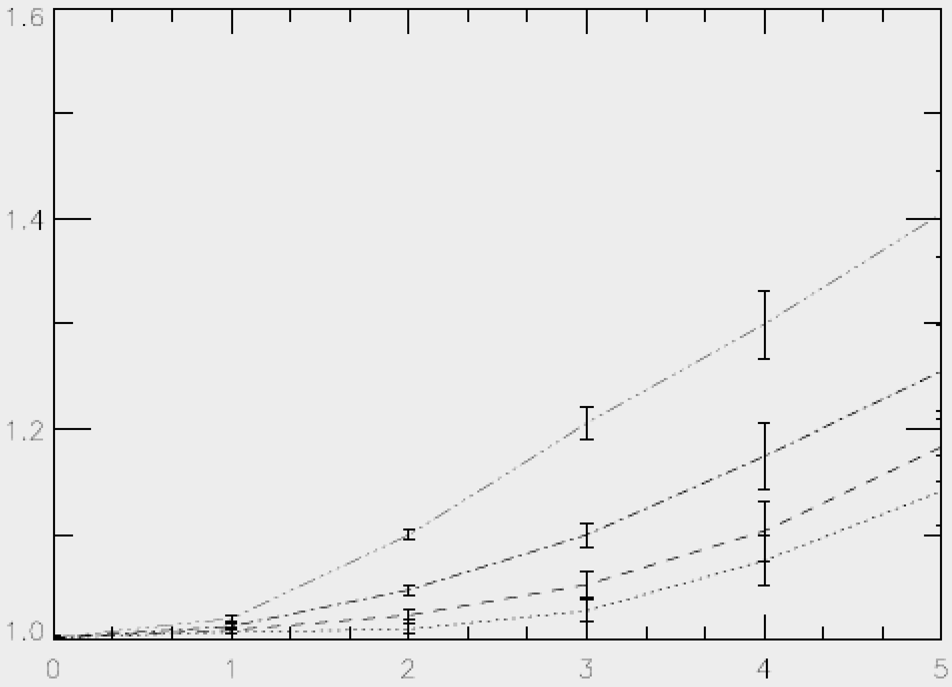

Fig. 7.11. Mean entropy (ordinate) versus scale (abscissa) of 5 simulated images containing undetectable sources and noise. Each curve corresponds to the multi-scale transform of one image. From top curve to bottom curve, the image contains respectively 400, 200, 100, 50 and 0 sources.

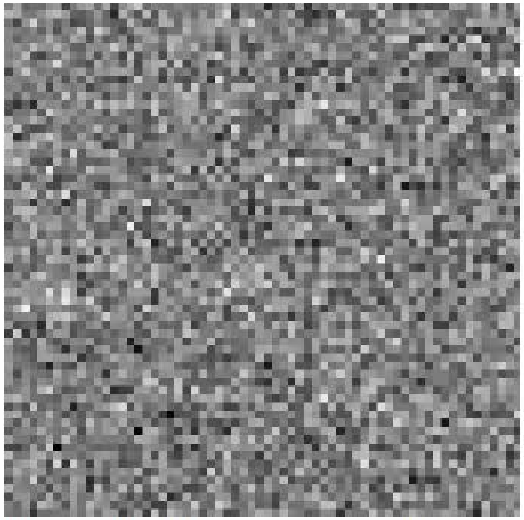

Fig. 7.12. Region of a simulated image containing an undetectable source at the center.

Compressed Sensing

Compressed Sensing

Sample-Then-Compress Paradigm

- Standard digital data acquisition paradigm
  - *sample* (ADC, digital camera, ...)
  - *compress* (signal-dependent, nonlinear)

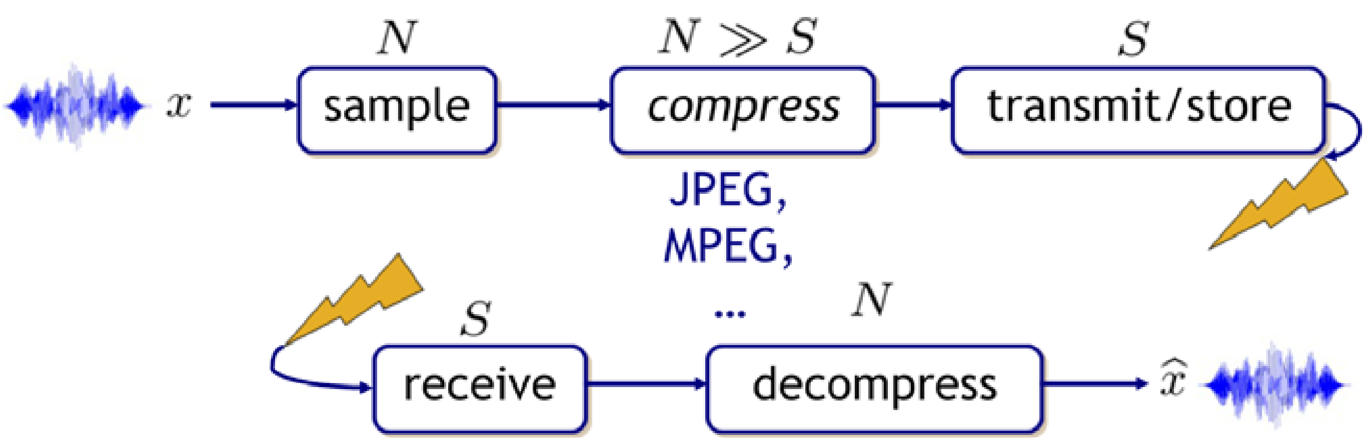

Compressed Sensing

Original image

Jedes Pixel entspricht einer „Messung“

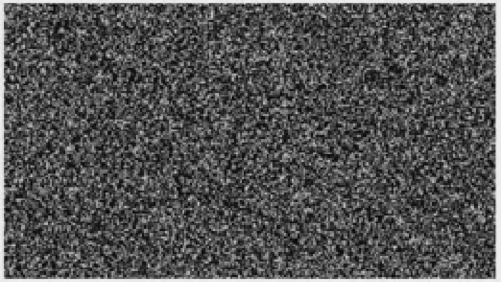

Linear combinations
of pixels

Anstatt alle Pixel eines Bildes aufzunehmen, werden nur Linearkombinationen dieser Pixel aufgezeichnet (Messung)

Compressed Sensing

>

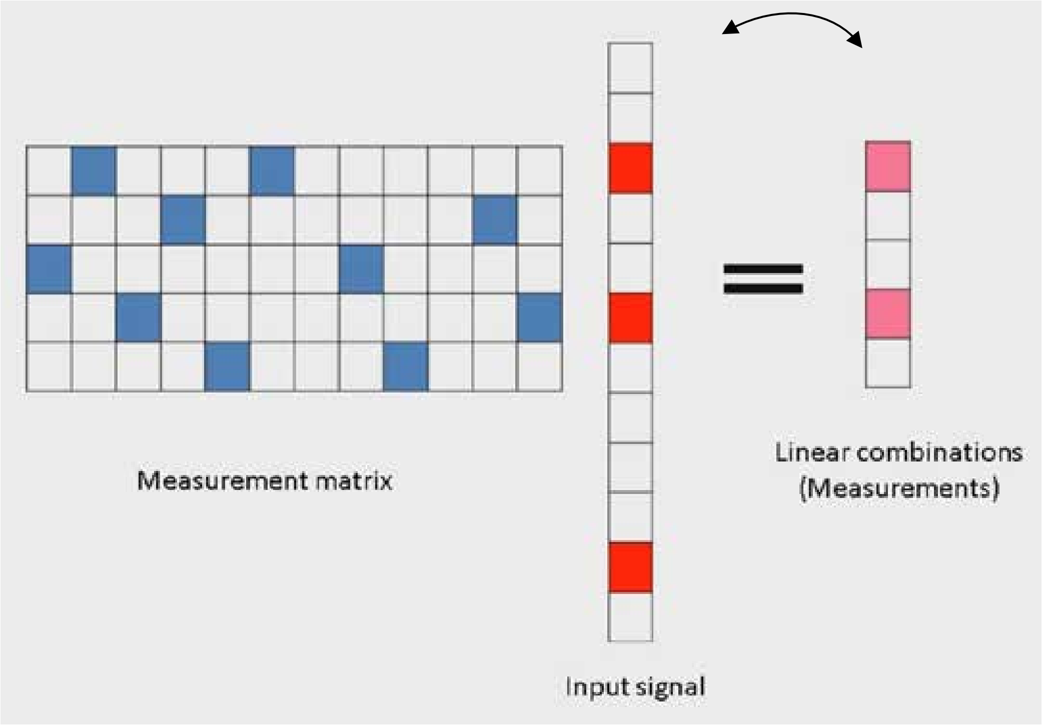

Anstatt alle Pixel eines Bildes aufzunehmen, werden nur Linearkombinationen dieser Pixel aufgezeichnet (Messung)

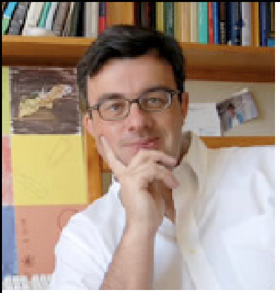

Compressed Sensing

* E. Candès and T. Tao, "Near Optimal Signal Recovery From Random Projections: Universal Encoding Strategies? ", IEEE Trans. on Information Theory, 52, pp 5406-5425, 2006.
* D. Donoho, "Compressed Sensing", IEEE Trans. on Information Theory, 52(4), pp. 1289-1306, April 2006.
* E. Candès, J. Romberg and T. Tao, "Robust Uncertainty Principles: Exact Signal Reconstruction from Highly Incomplete Frequency Information", IEEE Trans. on Information Theory, 52(2) pp. 489 - 509, Feb. 2006.

A non linear sampling theorem

"Signals with exactly K components different from zero can be recovered perfectly from ~ K log N incoherent measurements"

Replace samples with *few linear projections* $y = \Theta x$

$M \times 1$ measurements

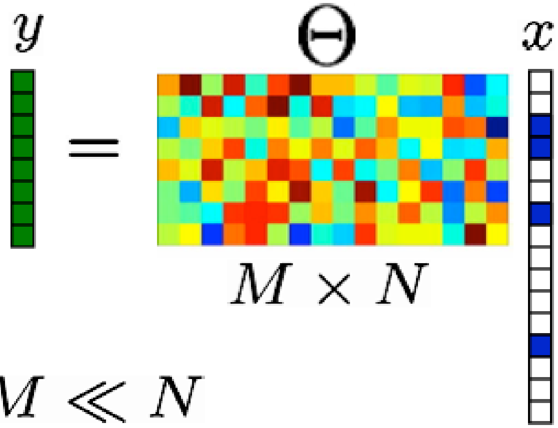

$N \times 1$ sparse signal

$y_k = \langle x, \theta_k \rangle$

K nonzero entries

$K < M \ll N$

Reconstruction via non linear processing:

$$\min_x \|x\|_1 \quad \text{s.t.} \quad y = \Theta x$$

Conditions on the sensing matrix to get stable and robust recovery (RIP)

$\Rightarrow$Application: Compression, tomography, ill posed inverse problem.

Compressed Sensing

Single Pixel Camera (RICE University)

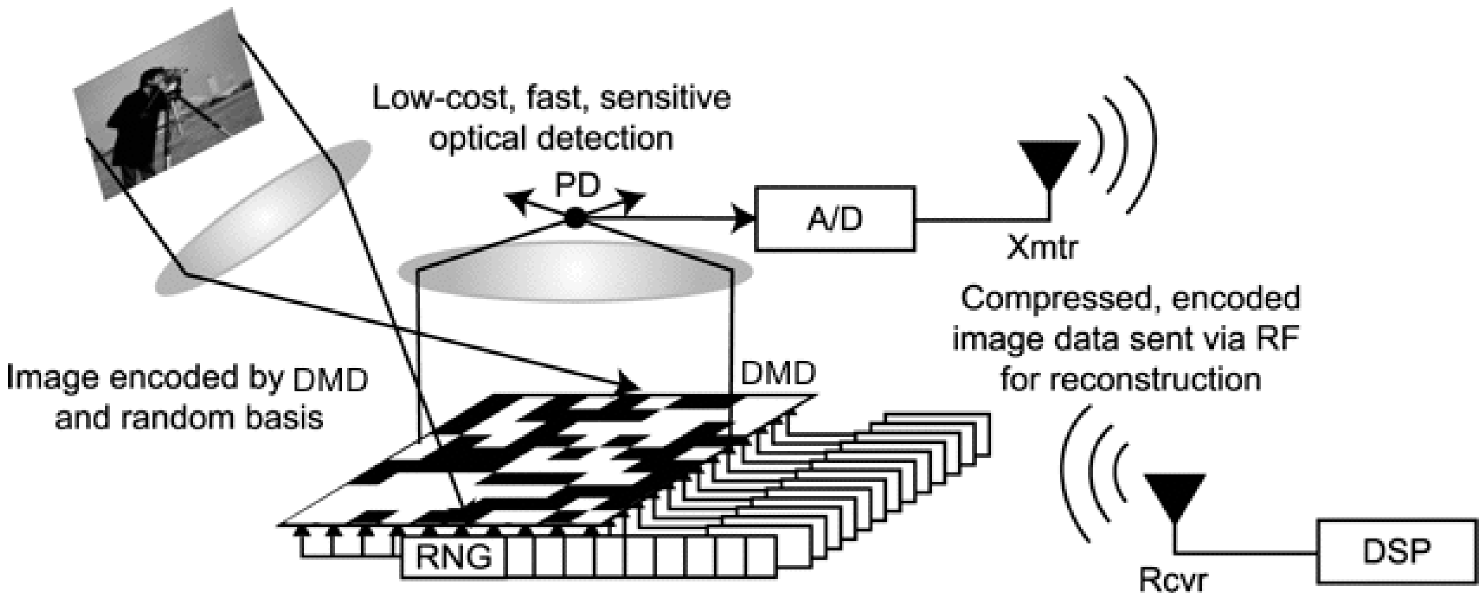

Compressed Sensing

„Inpainting“

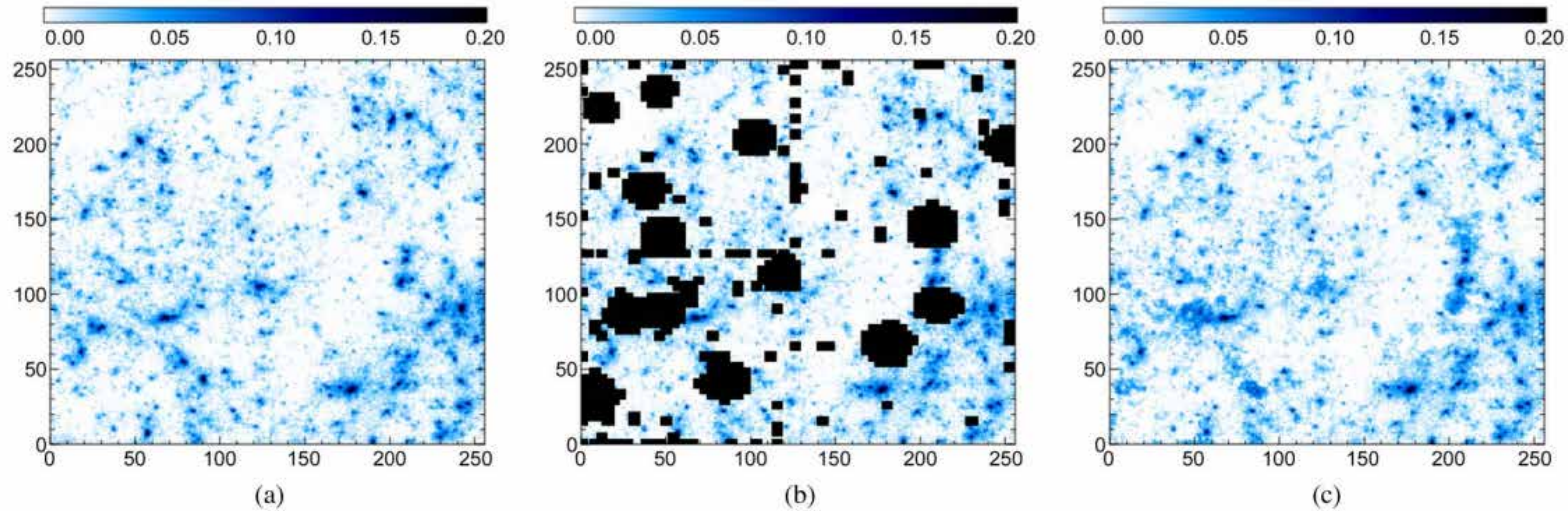

Fig. 5. ***(a) Simulated weak lensing mass map, (b) simulated mass map with a standard mask pattern, and (c) inpainted mass map. The region shown is $1^\circ \times 1^\circ$.***

Compressed Sensing

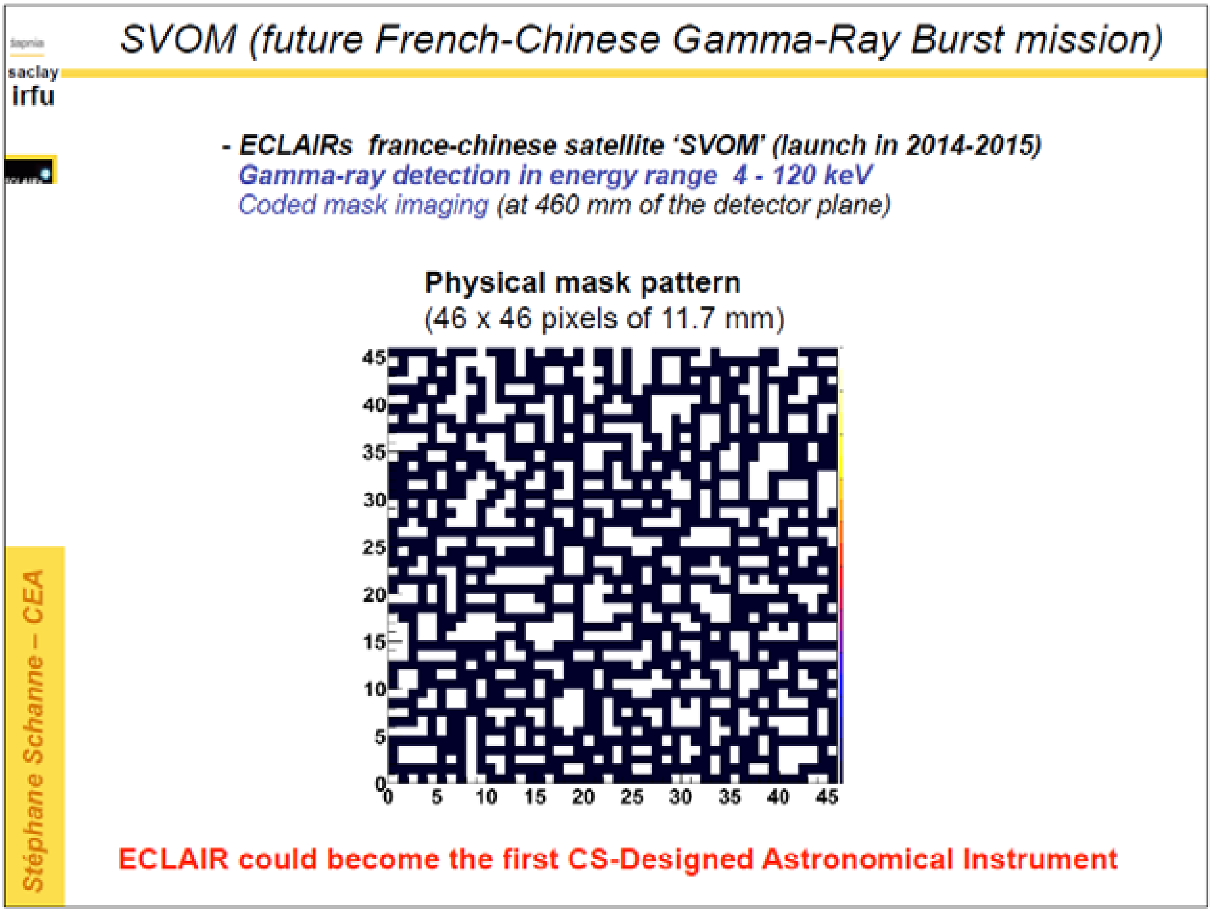

http://astrostat.sciencesconf.org/3093/document